CANCER

A chimeric antigen receptor with antigen-independent OX40 signaling mediates potent antitumor activity

Huihui Zhang[1,2,3]*, Fanlin Li[1,2,3]*, Jiang Cao[4]*, Xin Wang[5], Hai Cheng[4], Kunming Qi[4], Gang Wang[6], Kailin Xu[4], Junnian Zheng[6], Yang-Xin Fu[7], Xuanming Yang[1,2,3]†

Although chimeric antigen receptor (CAR)–modified T cells have shown great success in the treatment of B cell malignancies, this approach has limited efficacy in patients with solid tumors. Various modifications in CAR structure have been explored to improve this efficacy, including the incorporation of two costimulatory domains. Because costimulatory signals are transduced together with T cell receptor signals during T cell activation, we engineered a type of CAR-T cells with a costimulatory signal that was activated independently from the tumor antigen to recapitulate physiological stimulation. We screened 12 costimulatory receptors to identify OX40 as the most effective CAR-T function enhancer. Our data indicated that these new CAR-T cells showed superior proliferation capability compared to current second-generation CAR-T cells. OX40 signaling reduced CAR-T cell apoptosis through up-regulation of genes encoding Bcl-2 family members and enhanced proliferation through increased activation of the NF-κB (nuclear factor κB), MAPK (mitogen-activated protein kinase), and PI3K-AKT (phosphoinositide 3-kinase to the kinase AKT) pathways. OX40 signaling not only enhanced the cytotoxicity of CAR-T cells but also reduced exhaustion markers, thereby maintaining their function in immunosuppressive tumor microenvironments. In mouse tumor models and in patients with metastatic lymphoma, these CAR-T cells exhibited robust amplification and antitumor activity. Our findings provide an alternative option for CAR-T optimization with the potential to overcome the challenge of treating solid tumors.

INTRODUCTION

T lymphocytes are critical immune cells for antitumor immunity. In solid tumors, the tumor microenvironment is often immunosuppressive, blocking the activity of antitumor T cells. Various strategies have been developed to reactivate endogenous antitumor T cells, but the generation of large numbers of antigen-specific T cells to effectively control tumor growth remains challenging (*1*, *2*). Alternative ways to engineer tumor-specific T cells ex vivo have been developed, and adoptive transfer of large numbers of tumor-reactive T cells into patients has shown promising outcomes in clinical settings (*3*). Chimeric antigen receptor (CAR)–engineered T cells were developed as a main cellular therapy through the generation of a large number of tumor-targeting T cells (*4*). A CAR consists of an extracellular antigen-binding domain, a hinge, a transmembrane domain, and intracellular domains with a costimulatory domain from a costimulatory receptor, such as 4-1BB, and an activation domain from the T cell receptor (TCR) complex protein CD3ζ (*5*). Despite the antitumor efficacy of CAR-T cells in treating B cell–derived leukemia, the efficacy of these cells for the treatment of lymphoma or solid tumors is limited (*6*, *7*). Numerous technical and biological obstacles have limited the success of using CAR-T cells for the treatment of solid tumors, such as poor T cell persistence, development of T cell exhaustion, insufficient homing of infused T cells to tumor sites, and impaired function within the immunosuppressive tumor microenvironment (*6*–*8*).

The molecular design of CARs is likely to strongly influence the expansion and persistence of this population of T cells, as well as control CAR-T cell function in vivo. The enhancement of antitumor activity of CAR-T cells is a focus of intensive research efforts (*3*, *7*). Strategies to improve antigen recognition, trafficking into tumors, and persistence within tumors and to counter the tumor microenvironment are urgently needed to develop CAR-T cells as solid tumor therapies (*3*, *6*–*9*). Various approaches strive to resolve these limitations (*10*–*14*). CAR-T cells engineered to produce the T cell zone maintenance cytokine interleukin-7 (IL-7) and chemokine CCL19 have induced complete regression of solid tumors in a mouse model (*10*). These IL-7– and CCL19-producing CAR-T cells not only show robust persistence within the tumor themselves but also recruit and activate endogenous dendritic cells and T cells to the tumor (*10*). To overcome immune suppression from tumor microenvironments, CAR-T cells engineered to produce a single-chain variable antibody fragment against the immune checkpoint inhibitor receptor PD-1 (scFv–anti–PD-1) (*13*) exhibit enhanced antitumor activity in vitro and in vivo. The secreted scFv–anti–PD-1 changes the tumor microenvironment and promotes endogenous antitumor T cell responses in a paracrine manner (*13*). To reduce on-target but off-tumor toxicities of CAR-T cells, T cells activated by a tumor-specific pattern were designed by engineering the cells with a trio of chimeric receptors that mimic physiologic T cell signaling by simultaneously providing TCR activation, costimulation, and a third cytokine signal (*11*).

Costimulation signaling pathways are important for T cell activation and proliferation (*15*, *16*). Distinct costimulatory signals are used by different stages and subtypes of T cells (*15*, *17*). Some costimulatory receptors belong to the tumor necrosis factor receptor (TNFR) superfamily: TNFR2, OX40 (CD134), 4-1BB (CD137), herpes virus entry mediator (HVEM), CD27, and death receptor 3 (DR3) (*17*). These receptors recruit adaptor proteins of the TNFR-associated

[1]Sheng Yushou Center of Cell Biology and Immunology, School of Life Sciences and Biotechnology, Shanghai Jiao Tong University, Shanghai 200240, China. [2]Joint International Research Laboratory of Metabolic and Developmental Sciences, Shanghai Jiao Tong University, Shanghai 200240, China. [3]Key Laboratory of Systems Biomedicine (Ministry of Education), Shanghai Center for Systems Biomedicine, Shanghai Jiao Tong University, Shanghai 200240, China. [4]Department of Hematology, Affiliated Hospital of Xuzhou Medical University, Xuzhou 221002, China. [5]Shanghai Longyao Biotechnology Limited, Shanghai 201203, China. [6]Cancer Institute, Xuzhou Medical University, Xuzhou 221002, China. [7]Department of Pathology, University of Texas Southwestern Medical Center, Dallas, TX 75390, USA.
*These authors contributed equally to this work.
†Corresponding author. Email: xuanmingyang@sjtu.edu.cn

factor (TRAF) family and activate the NF-κB (nuclear factor κB) pathway (*18*, *19*). OX40 is not present on naïve T cells but is rapidly induced after T cell activation (*20*). OX40 activation by the ligand OX40L has broad effects on T cell activation, proliferation, differentiation, and survival (*21*–*24*). OX40 delivers a costimulatory signal that activates $CD4^+$ T cells, promoting expansion and survival of this effector T cell population (*21*, *24*) and inducing the generation of memory $CD4^+$ T cells (*22*). OX40 activation also supports T helper 2 (T_H2) and T_H9 cell differentiation (*22*, *23*, *25*). At the molecular level, OX40 signaling recruits TRAF2, TRAF3, or TRAF5 to activate NF-κB

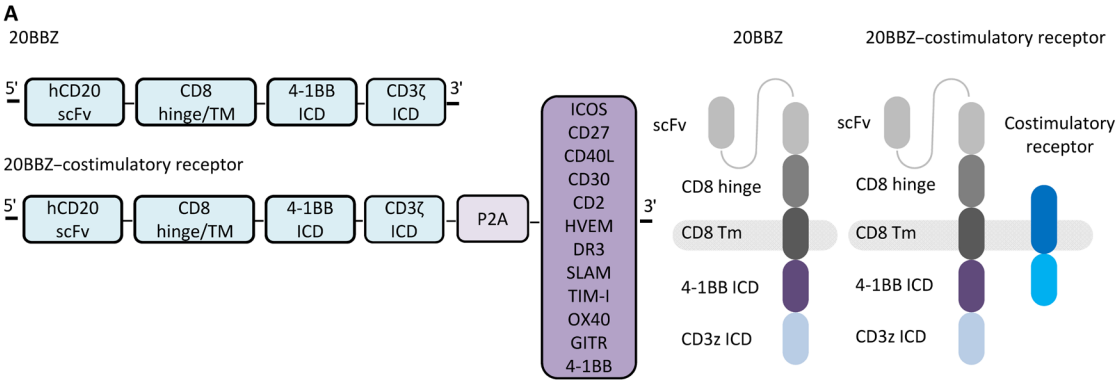

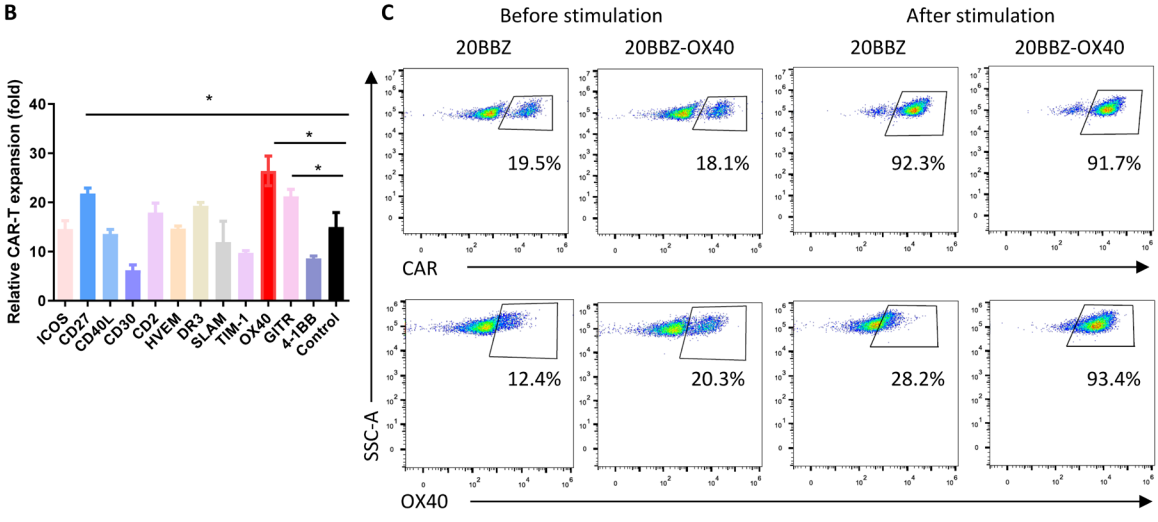

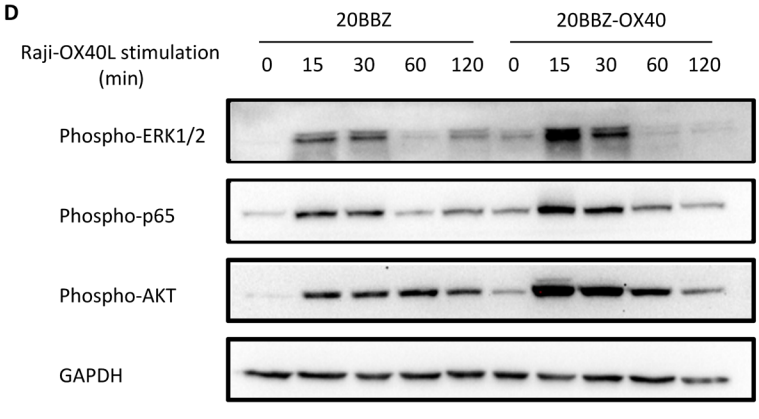

Fig. 1. Systemic screening identifies OX40 as a potential CAR function enhancer. (**A**) Schematic diagram of the CD20-targeting CAR constructs used in this study. An scFv against human CD20 was linked to 4-1BB and CD3ζ to generate a 20BBZ construct. Various costimulatory receptors were linked to CD3ζ through a P2A sequence. TM, transmembrane domain; ICD, intracellular domain. (**B**) The relative proliferation of CAR-T cells expressing a CAR with 1 of 12 costimulatory receptors at day 7 after lentiviral transduction. Fold change in CAR-T cell numbers was calculated by dividing the cell number on day 7 over the cell number on day 1. Data are presented as means ± SEM from one of two experiments with statistical significance determined by unpaired *t* test. The normality of data was confirmed by Shapiro-Wilk test. Statistical significance was presented by $*P < 0.05$. (**C**) Flow cytometry analysis of the proportion of cells positive for CAR (top) or OX40 (bottom) in T cells expressing 20BBZ or 20BBZ-OX40. Cells were stimulated with irradiated Raji cells four times every 6 days. Representative results from one of four experiments are shown. (**D**) Western blot analysis of phosphorylated p65, ERK, and AKT in 20BBZ and 20BBZ-OX40 CAR-T cells. CAR-T cells were stimulated with OX40L-overexpressing Raji-OX40L cells for 15, 30, 60, and 120 min. Phosphorylated ERK1/2, p65, and AKT were detected by immunoblotting. GAPDH was used as a loading control. Representative results from one of four repeated experiments are shown.

and induce antiapoptotic gene expression (*21*, *26*, *27*), as well as promotes the PI3K/AKT (phosphoinositide 3-kinase to AKT) pathway to enhance cell survival and cell cycle progression (*24*, *28*, *29*). Furthermore, OX40 signaling enhances the expression of genes encoding proinflammatory effector molecules and proteins that promote cell proliferation through activation of the transcription factor NFAT (*23*, *30*). In natural T cells, costimulatory signals, such as the OX40 signal, are delivered through a separate receptor from the TCR and are independent of TCR engagement, whereas in CAR-modified T cells, this signal occurs upon antigen recognition. The effect of

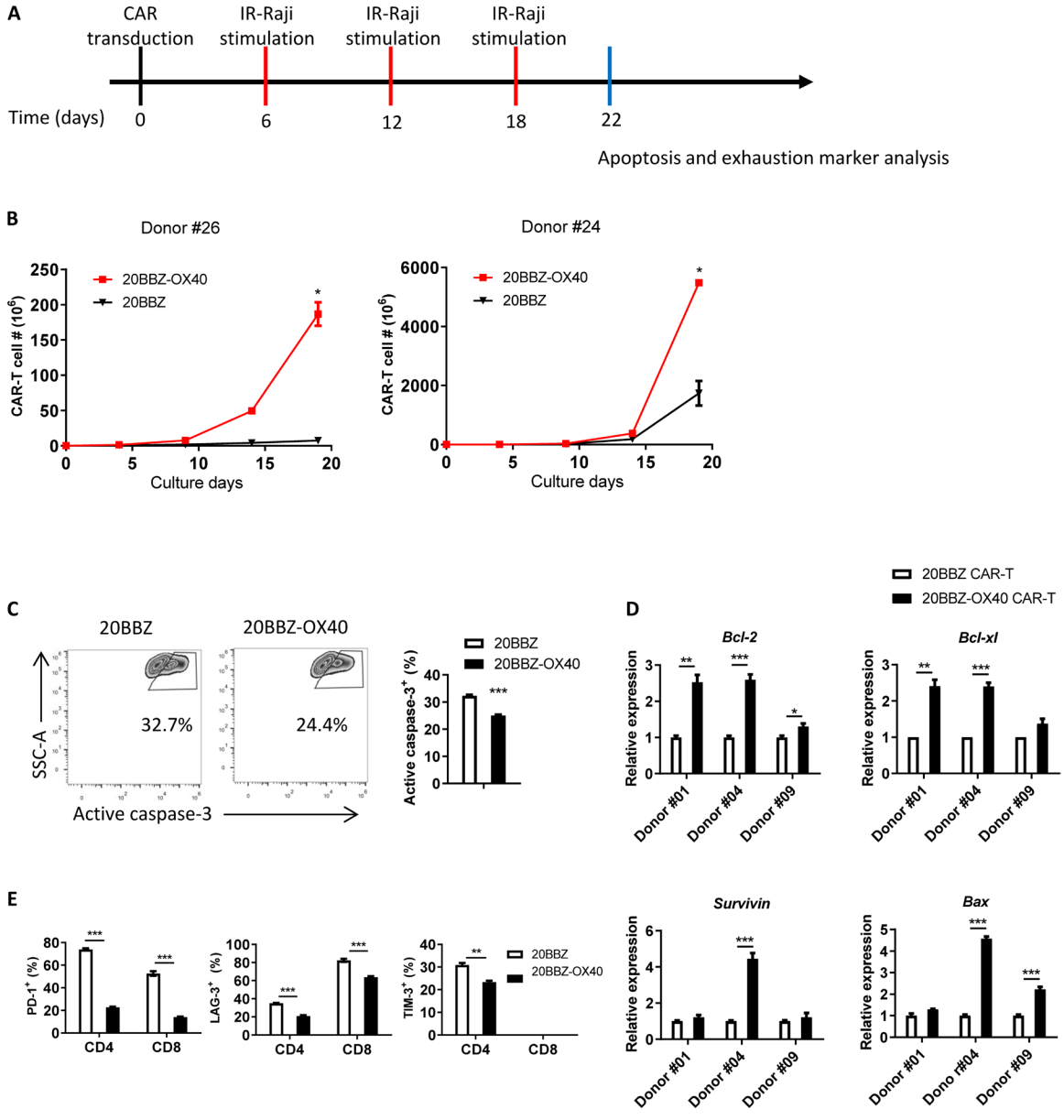

Fig. 2. OX40 signaling enhanced CAR-T cell proliferation and reduced apoptosis. (**A**) Schematic diagram of the long-term CAR-T population expansion assay. T cells were infected with indicated CAR lentivirus and stimulated by coculture with irradiated (IR) Raji cells once every 6 days. Total cell number was recorded, and CAR^+ cell percentage was analyzed by flow cytometry. (**B**) CAR^+ T cells in cultures of 20BBZ- or 20BBZ-OX40–expressing CAR-T cells. Experiments were repeated with T cells from two different donors. Results from two of five experiments are shown. Statistical significance was determined by Mann-Whitney *U* test and presented by $^*P < 0.05$. (**C**) Analysis of apoptotic CD20BBZ and CD20BBZ-OX40 CAR-T cells on day 22 after stimulation with irradiated Raji cells. Apoptotic cells were detected by flow cytometry of cells stained for active caspase-3. Results from two independent experiments with two different donors are shown. (**D**) Analysis of mRNA expression of *Bcl-2*, *survivin*, *Bax*, and *Bcl-xL* in T cells expressing 20BBZ or 20BBZ-OX40 CAR constructs on day 22 after stimulation with irradiated Raji cells. GAPDH was used as a control. Data were acquired by quantitative reverse transcription PCR and are presented as relative to 20BBZ samples. Results from one of two independent experiments are shown. (**E**) Percentage of $CD4^+$ or $CD8^+$ CAR-T cells positive for cell surface markers of T cell exhaustion (PD-1, LAG-3, and TIM-3) on day 22 after stimulation with irradiated Raji cells. Representative results from one of three repeated experiments are shown. (C to E) Data are presented as means ± SEM with statistical significance determined by unpaired *t* test. The normality of data was confirmed by Shapiro-Wilk test. Statistical significance was presented by $^*P < 0.05$, $^{**}P < 0.01$, and $^{***}P < 0.001$.

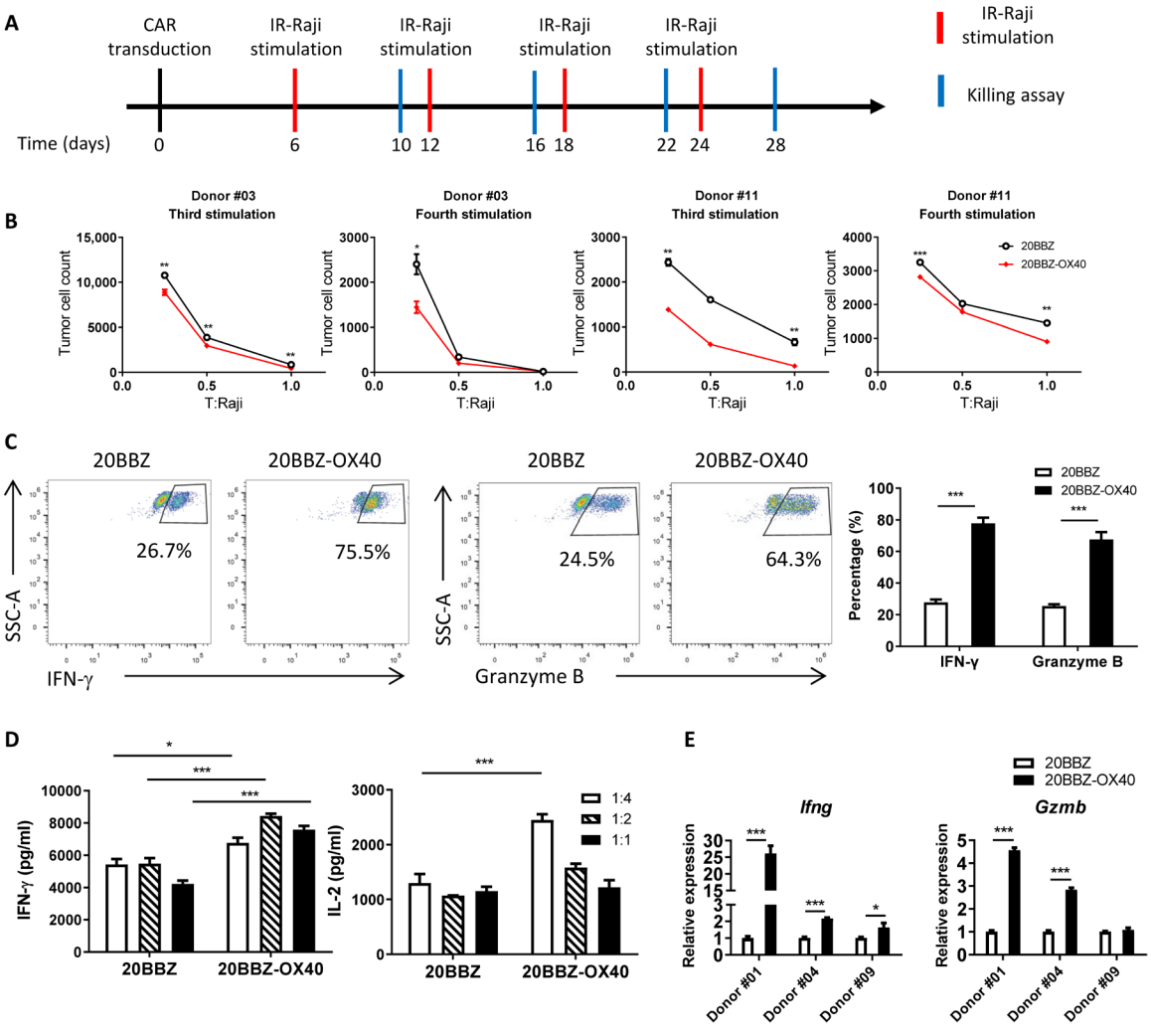

Fig. 3. 20BBZ-OX40 CAR-T cells have cytotoxic activity after repetitive antigen stimulation. (**A**) Schematic diagram of the CAR-T cell cytotoxicity assay after long-term repetitive antigen stimulation. T cells were transduced with the indicated CAR lentivirus constructs and stimulated with irradiated Raji cells once every 6 days. On day 4 after each stimulation, CAR-T cells were used in the cytotoxicity assay. (**B**) 20BBZ and 20BBZ-OX40 CAR-T cells generated from T cells from the indicated donors were cocultured with Raji cells in triplicate at the different effector:target (T cell:Raji cell) ratios for 24 hours. Remaining Raji cells ($CD3^-CD19^+$) were determined by flow cytometry as an indicator of cytotoxicity. Data are presented as means ± SEM and are the results of two of four experiments. Statistical significance was determined by unpaired *t* test. The normality of data was confirmed by Shapiro-Wilk test. (**C**) 20BBZ and 20BBZ-OX40 CAR-T cells were cocultured with Raji cells for 72 hours. Representative intracellular staining of IFN-γ and granzyme B in 20BBZ and 20BBZ-OX40 CAR-T cells (left) and summarized data (right) are shown. Data are presented as means ± SEM and are one result of two experiments. Statistical significance was determined by unpaired *t* test. The normality of data was confirmed by Shapiro-Wilk test. (**D**) 20BBZ and 20BBZ-OX40 CAR-T cells were cocultured with Raji cells for 24 hours. Cytokines secreted by 20BBZ and 20BBZ-OX40 CAR-T cells were measured determined by Cytometric Bead Array (CBA) assay. Data are presented as means ± SEM and are the results of one of four experiments. Statistical significance was determined by unpaired *t* test. The normality of data was confirmed by Shapiro-Wilk test. (**E**) Analysis of mRNA expression of genes encoding IFN-γ (*Ifng*) and granzyme B (*Gzmb*) in 20BBZ and 20BBZ-OX40 CAR-T cells. Data are presented as means ± SEM of values relative to 20BBZ samples and are the results of one of three experiments. Statistical significance was determined by unpaired *t* test. The normality of data was confirmed by Shapiro-Wilk test. (**F**) 20BBZ and 20BBZ-OX40 CAR-T cells were cocultured with 1×10^5 Nalm-6 cells or Nalm-6 cells expressing hCD20. Cytotoxicity was determined by analyzing the remaining Nalm-6 or Nalm-6-hCD20 cells ($CD3^-CD19^+$) by flow cytometry. Data are presented as means ± SEM and are the results of one of three experiments. Statistical significance was determined by unpaired *t* test. The normality of data was confirmed by Shapiro-Wilk test. Statistical significance was presented by $^*P < 0.05$, $^{**}P < 0.01$, and $^{***}P < 0.001$. NS, not significant.

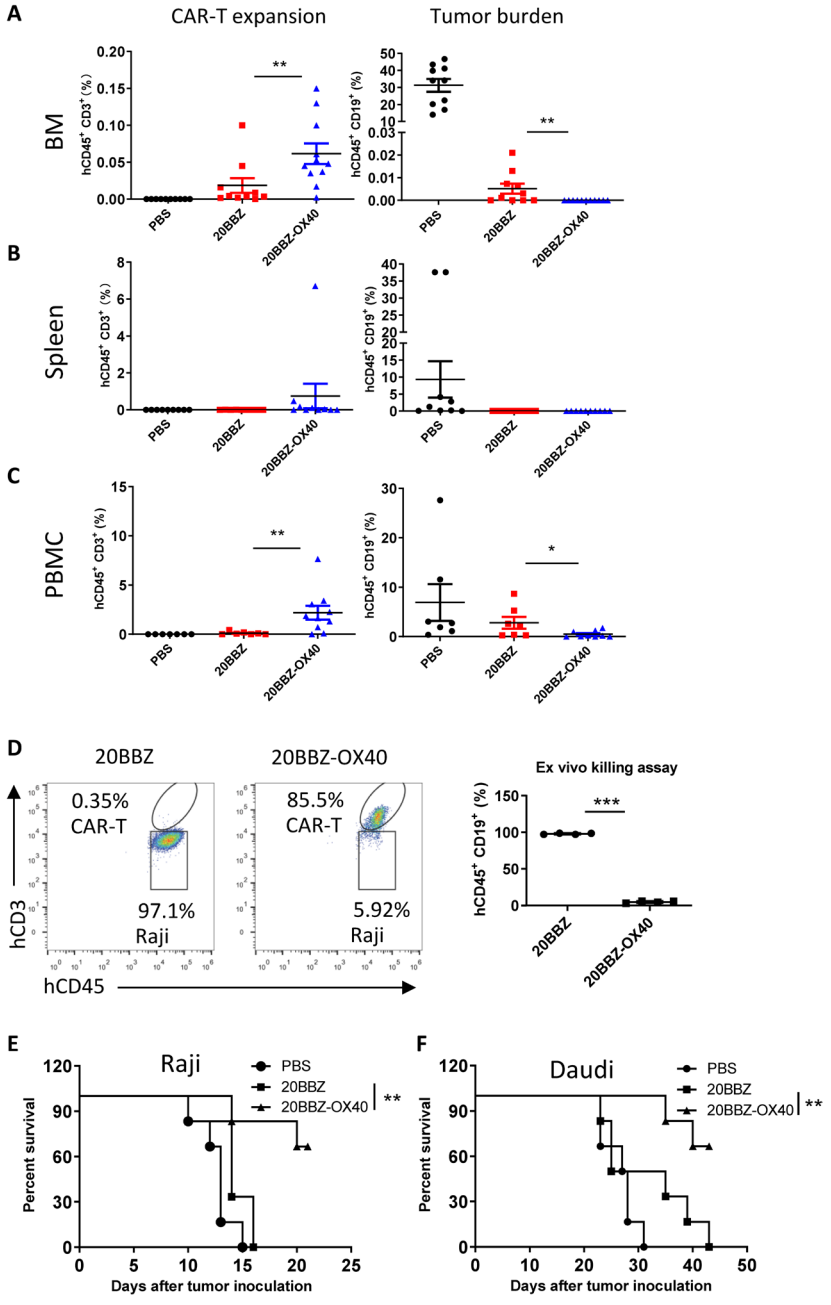

Fig. 4. 20BBZ-OX40 CAR-T cells persist and demonstrate antitumor function in vivo. (**A** to **C**) NSG mice were intravenously inoculated with of 1×10^6 Raji cells. Seven days later, tumor-bearing mice were treated with 1×10^7 20BBZ or 20BBZ-OX40 CAR-T cells. Seven days after the treatment, bone marrow (BM) (A), spleen (B), and peripheral blood mononuclear cells (PBMCs) (C) were collected for analysis of CAR-T cells ($mCD45^-hCD45^+hCD3^+$) and Raji ($mCD45^-hCD45^+ hCD19^+$) tumor cell burden. Data are presented as means ± SEM and are the results of two of three experiments, $n = 9$ to 11 per group for bone marrow and spleen samples and $n = 7$ to 10 per group for blood samples. Statistical significance was determined by Mann-Whitney *U* test and presented by $^*P < 0.05$ and $^{**}P < 0.01$. (**D**) Seven days after treatment, bone marrow–derived cells from tumor-bearing mice were cultured ex vivo. Raji cells were added to the culture at an effector:target ratio of 2:1. Seven days after culture, CAR-T cells ($mCD45^-hCD45^+hCD3^+$) and Raji cells ($mCD45^-hCD45^+ hCD19^+$) were analyzed by flow cytometry to evaluate Raji cell killing. Data are presented as means ± SEM and are the results of one of two experiments. Statistical significance was determined by unpaired *t* test and presented by $^{***}P < 0.001$. The normality of data was confirmed by Shapiro-Wilk test. (**E** and **F**) NSG mice were intravenously inoculated with 1×10^6 Raji (E) or 1.5×10^6 Daudi (F) tumor cells. Seven days later, tumor-bearing mice were treated with 1×10^7 20BBZ or 20BBZ-OX40 CAR-T cells or PBS ($n = 6$ mice per group). Kaplan-Meier curves for overall survival of the mice are shown. Representative results of one from three (E) and two (F) repeated experiments are shown. Statistical significance was determined by Mantel-Cox test, presented by $^*P < 0.05$, $^{**}P < 0.01$, and $^{***}P < 0.001$.

including a costimulatory signal that is activated independently from the antigen-mediated activation of the CAR-T cell has not been systemically investigated.

In this study, we established a CAR-T cell structure with not only an intracellular signaling domain from a costimulatory protein that requires antigen engagement of the CAR for activation but also includes a constitutively expressed full-length costimulatory receptor component that is activated by its natural costimulatory ligand. Current clinically used CARs include a costimulatory domain from 4-1BB that is adjacent to the CD3ζ activation domain from the TCR complex and is activated by antigen recognition (*31*). By screening 12 costimulatory receptors, we identified OX40 as an effective CAR-T cell function enhancer when incorporated into the standard clinically used 4-1BB domain–based CAR construct. In this 20BBZ-OX40 construct, full-length OX40 is coexpressed with a second-generation CAR recognizing CD20 and thus depends on endogenous costimulatory ligand engagement rather than antigen recognition for activation. The 20BBZ-OX40 CAR-T cells showed enhanced proliferation, improved tumor killing, and less exhaustion compared with the widely used 20BBZ-based CAR-T cells that only include the costimulatory domain from 4-1BB. Furthermore, the antitumor activity and persistence of the 20BBZ-OX40 CAR-T cells were greatly enhanced in mouse tumor models, whereas the BBZ-based CAR-T cells showed minimal activity. 20BBZ-OX40 CAR-T cells exhibited robust amplification and potent antitumor activity in clinical trials in patients with B cell lymphoma without causing severe side effects. This work provides evidence for a strategy for optimizing the function of CAR-T cells.

RESULTS

OX40 was identified as a potential CAR function enhancer via a systemic screening approach.

In current CAR therapeutic design for clinical use, costimulatory signals are activated with CAR signaling upon antigen recognition. However, during natural T cell activation, the costimulatory signal is transduced in parallel with the TCR signal. To test whether CAR-T cells benefit from additional antigen-independent

costimulatory signals, we performed a systemic screen of 12 costimulatory receptors to identify potential CAR function enhancers. We generated a lentiviral vector that encoded an scFv against hCD20, a CD8 hinge and transmembrane domain, an intracellular region with 4-1BB and CD3ζ domains, a P2A peptide (ATNFSLLKQAGDVEENPGP), and various intact full-length costimulatory receptors: inducible T cell co-stimulator (ICOS), CD27, CD40L, CD30, CD2, HVEM, DR3, signaling lymphocyte activation molecule, T cell immunoglobulin and mucin domain–containing molecule-1 (TIM-1), OX40, 4-1BB, or glucocorticoid-induced TNFR (GITR) (Fig. 1A and table S1). The P2A-based multicistronic protein expression is mediated by ribosome skipping (*32*). This fusion DNA is transcribed to an intact mRNA through the classical transcription machinery. During subsequent translation, 20BBZ polypeptides break from indicated costimulatory receptors between glycine and proline in the P2A region. This process resulted in two separate proteins: the 20BBZ CAR and a full-length costimulatory receptor. We used the 4-1BB–based CAR (20BBZ) as a control (Fig. 1A). We transduced human T cells with these lentiviruses and compared proliferation of the T cells in culture. After a 7-day culture period, we observed a significant growth enhancement of T cells expressing 20BBZ-GITR, 20BBZ-CD27, or 20BBZ-OX40 compared with growth of control 20BBZ CAR-T cells ($P < 0.05$; Fig. 1B), with OX40-expressing CAR-T cells showing the greatest increase in proliferation. Thus, we focused on characterizing the OX40-containing CAR-T cells.

To evaluate potential sources of OX40L for activation of OX40 signaling, we first determined the abundance of OX40L on 20BBZ CAR-T cells, donor T cells, and three leukemia or lymphoma cell lines ($CD19^+$ Nalm-6 cells, $CD20^+$ Raji cells, and $CD20^+$ Daudi cells). Both Raji and Daudi tumor cells had abundant OX40L (fig. S1), thereby providing a source for activation of OX40. We detected a similar CAR^+ proportion of 20BBZ and 20BBZ-OX40 cells, and after repeated stimulation with irradiated $CD20^+$ Raji cells, the percentage of the CAR^+ T cells reached ~90% from an initial ~20% (Fig. 1C). These results suggested that both CARs were functionally expressed and transduced activation and proliferation signals in T cells. In 20BBZ CAR-T cells, the percentage of cells positive for OX40 was low (12.4% OX40 positive before stimulation and 28.2% positive after stimulation), whereas the proportion of T cells positive for the CAR and OX40 was similar in the absence of Raji cells and after stimulation, indicating the simultaneous expression of OX40 and CAR in 20BBZ-OX40 CAR-T cells (Fig. 1C).

OX40 transduces activating signals to NF-κB, extracellular signal–regulated kinases (ERK1 and ERK2) in the mitogen-activated protein kinase (MAPK) pathway, and AKT in the PI3K pathway (*33*). To assess whether OX40 signaled through all of these pathways in 20BBZ CAR-T cells, we compared the phosphorylation of ERK, p65 (a subunit of NF-κB), and AKT in 20BBZ-OX40 and 20BBZ CAR-T cells. After incubation with OX40L-overexpressing Raji cells, phospho-AKT, phospho-ERK1/2, and phospho-p65 appeared to have increased in 20BBZ-OX40 CAR-T cells compared with the amounts in 20BBZ cells (Fig. 1D). These results suggested that the constitutively expressed OX40 in CAR-T cells is functional and that OX40 signaling may provide growth and activation benefits for CAR-T cells.

We observed that 20BBZ-OX40 CAR-T cells had enhanced activity through multiple signal pathways (Fig. 1D). To test the relevance of these pathways for enhancing OX40-mediated CAR-T cell proliferation, we evaluated the proliferation of 20BBZ-OX40 CAR-T cells in the presence of small-molecule inhibitors. First, we tested whether the small-molecular inhibitors specifically reduced activation of the appropriate pathway in 20BBZ-OX40 CAR-T cells (fig. S2). We found that two (ravoxertinib and ulixertinib) of the four ERK1/2 inhibitors increased, rather than decreased, ERK1/2 phosphorylation. In addition, the AKT inhibitor afuresertib increased AKT phosphorylation, and PI3K inhibitor wortmannin reduced ERK1/2 phosphorylation. These observations are consistent with previous publication (*34*–*40*). Ravoxertinib (*34*), ulixertinib (*35*, *36*), and afuresertib (*37*, *38*) increase the phosphorylation of their targets possibly through a feedback loop while do not affect their inhibitory effect on the phosphorylation of their substrates. Wortmannin inhibits the phosphorylation of ERK1/2 by an unknown mechanism (*39*, *40*). We evaluated a pair of inhibitors for each pathway and found that each reduced proliferation of Raji cell–stimulated 20BBZ-OX40 CAR-T cells compared with the proliferation of cells stimulated in the presence of vehicle (fig. S3). Collectively, these results suggested that these cells respond to tumor cells by activating a complex network and that each part of the network contributes to their proliferation.

Full-length OX40 enhanced CAR-T cell proliferation in the context of multiple CAR constructs

In vivo, OX40 signaling enhances the expansion of the T cell population after antigen recognition (*41*). We investigated whether activation of OX40 signaling by tumor cells contributes to proliferation and survival of CAR-T cells in culture. To mimic the long-term exposure of CAR-T cells in tumor-bearing host in vivo, we developed a repetitive antigen stimulation protocol using irradiated Raji cells (Fig. 2A). We examined the effect of this repetitive stimulation on CAR^+ cells generated with T cell from multiple donors and found that the 20BBZ-OX40 cells showed enhanced proliferation compared with that of 20BBZ cells (Fig. 2B and fig. S4).

We also compared the proliferation of 20BBZ-OX40 CAR-T cells to CAR-T cells with CAR constructs that contained the OX40 intracellular signaling domain integrated either before (20OXBBZ) or after (20BBOXZ) the 4-1BB domain in the intracellular portion of the CAR (third-generation CARs) (fig. S5A). Using repetitive antigen stimulation with irradiated Raji cells, 20BBZ-OX40 CAR-T cells showed enhancement of proliferation compared to either 20BBOXZ or 20OXBBZ CAR-T cells (fig. S5B). Because various factors, such as the relative position of the costimulation domains and the sequence and length of the linkers between costimulation domains, the CD3ζ domain, and hinge domain, could affect the function of the third generation of CAR-T cells (*42*), further optimization is required for the integration of the OX40 signaling domain into a third-generation CAR design.

To test whether expression of full-length OX40 promotes CAR-T cell proliferation in the absence of the 4-1BB costimulation domain, we established CAR-T cells with CAR constructs expressing only the scFv against hCD20, a CD8 hinge and transmembrane domain, and an intracellular region with the CD3ζ domain (20Z) and this construct with the P2A sequence and full-length OX40 (20Z-OX40). We compared the proliferation of T cells expressing these CAR constructs to 20BBZ CAR-T cells and found that only the 20BBZ-expressing cells showed pronounced proliferation, suggesting that the 4-1BB domain is important for cellular proliferation and that enhanced proliferation from adding full-length OX40 requires a combination of signals from the 4-1BB domain and OX40 signaling (fig. S6, A and B).

To test whether expression of OX40 enhances the function of CAR-T cells against other targets, we established CAR constructs with the scFv against hCD19 in the BBZ CAR context (19BBZ) and 19BBZ-OX40. Consistent with the data obtained with 20BBZ-OX40 CAR-T cells, 19BBZ-OX40 CAR-T cells showed greater proliferation and comparable cytotoxicity as compared to 19BBZ CAR-T cells (fig. S7, A to C). To test whether overexpression of OX40 enhances the function of other second generation of CAR-T cells, we established CAR constructs incorporated with hCD28 intracellular domain (1928Z) and 1928Z-OX40. However, we did not observe enhanced proliferation of 1928Z-OX40 CAR-T cells (fig. S8, A and B).

Full-length OX40 reduces CAR-T cell apoptosis and exhaustion

To assess whether the increased proliferation was due to reduced T cell apoptosis, we performed annexin V and 7-aminoactinomycin D (7-AAD) staining in both 20BBZ and 20BBZ-OX40 CAR-T cells. Flow cytometric analyses showed increased annexin V^+/7-AAD^+ populations in the 20BBZ CAR-T cells compared to the 20BBZ-OX40 CAR- T cells ($P < 0.01$; fig. S9). Furthermore, the proportion of cells with active caspase-3, a key apoptosis trigger, was less for 20BBZ-OX40 CAR-T cells than for 20BBZ CAR-T cells ($P < 0.001$; Fig. 2C). To understand the molecular basis for these results, we analyzed the mRNA expression of genes encoding antiapoptotic proteins in 20BBZ and 20BBZ-OX40 CAR-T cells after the third stimulation with Raji cells. Consistent with the reduced apoptotic phenotype in 20BBZ-OX40 CAR-T cells, mRNA abundance for *Bcl-2*, *Survivin*, *Bcl-xL*, and *Bax*—all encoding antiapoptotic proteins—was up-regulated in 20BBZ-OX40 CAR-T cells, although there was some variability based on the T cell donor (Fig. 2D). Together, these findings indicated that full-length OX40 and its activation by OX40L on tumor cells induced antiapoptotic gene expression that supported the increased proliferation of CAR-T cells.

To determine whether incorporation of full-length OX40 altered the distribution of T cell subsets, we compared the composition of unstimulated and stimulated 20BBZ and 20BBZ-OX40 CAR-T cells. Memory T cell populations are important for CAR-T cell proliferation (*14*). We analyzed different memory subtypes in both 20BBZ and 20BBZ-OX40 CAR-T cells and found no difference in the composition of effector memory T cells ($CCR7^-CD45RO^+CD45RA^-$) or central memory T cells ($CCR7^+CD45RO^+CD45RA^-$) in unstimulated or repetitively stimulated cells (fig. S10). In addition, the proportion of $CD4^+$ and $CD8^+$ cells was also similar between 20BBZ and 20BBZ-OX40 CAR-T cells (fig. S11). These results suggested that, in our culture and stimulation conditions, the memory phenotype is not the determining factor for long-term T cell persistence.

Inducing T cell exhaustion is a key immune escape mechanism for tumor cells. To test whether OX40 signaling affects the exhaustion status of CAR-T cells, we examined the abundance of exhaustion-related cell surface markers PD-1, TIM-3, and LAG-3. After the third antigen stimulation by incubation with Raji cells, the proportion of cells positive for PD-1 and LAG-3 was lower for both $CD4^+$ and $CD8^+$ 20BBZ-OX40 CAR-T cells than for 20BBZ CAR-T cells (Fig. 2E). The proportion of cells positive for TIM-3 in $CD4^+$ 20BBZ-OX40 CAR-T cells was also lower than that in 20BBZ CAR-T cells; however, TIM-3 was not detected in $CD8^+$ CAR-T cells (Fig. 2E). The reduction of these immune checkpoint inhibitor proteins could contribute to higher numbers of functional T cells within a solid tumor microenvironment.

20BBZ-OX40 CAR-T cells have cytotoxic activity after repetitive antigen stimulation

The cytotoxic ability of CAR-T cells directly determines their antitumor activity. To test whether parallel OX40 signaling enhances the cytotoxicity of CAR-T cells at different activation stages, we used a repetitive antigen stimulation method to mimic long-lasting chronic tumor burden. In this assay, T cells were stimulated every 6 days with irradiated $CD20^+$ Raji cells four times, and the T cells were harvested 4 days after each stimulation and then incubated with live Raji cells at various T cell:Raji cell ratios (Fig. 3A). To avoid the influence of CAR^+ cell percentage differences on cytotoxicity, we performed the tumor killing assay after the third and fourth stimulations. In three of four donors, 20BBZ-OX40 CAR-T cells killed more tumor cells than 20BBZ CAR-T cells killed (Fig. 3B and fig. S12, A and B). These results suggested that expression of full-length OX40 increased the cytotoxic capacity of CAR-T cells

Table 1. Baseline characteristics of patients and clinical response after 20BBZ-OX40 CAR T cell therapy. Baseline characteristics of patients and clinical response after 20BBZ-OX40 CAR T cell therapy. F, female; DLBCL, diffuse large B cell lymphoma; GCB, Germinal center B-cell like; IPI score, International Prognostic Index score; M, male; CRS, cytokine release syndrome.

Patient #	Sex	Age (years)	Lymphoma type	Number of previous therapies	Disease stage	IPI score	Refractory status*	CAR-T cells infused (cells/kg)	Best response	Duration of response (d)†	CRS	Neurological toxicity
1	M	24	DCBCL	3	IVB	3	Refractory	1×10^6	PR	‡	Grade 2	None
2	M	56	DCBCL	4	IVB	2	Refractory	2×10^6	CR	227§	None	None
3	F	63	DCBCL	3	IIIA	4	Refractory	2×10^6	PR	182§	Grade 1	None
4	M	60	Non-GCB DCBCL	3	IIIB	2	Refractory	4×10^6	PR	119§	Grade 1	None
5	M	31	DCBCL	4	IVB	3	Refractory	4×10^6	CR	54§	None	None

*Disease was defined as refractory if a patient did not achieve partial or complete remission after the most recent chemotherapy. †Duration of response was defined as the time from the first documented response (complete or partial remission) to the date of relapse, initiation of new treatment, or death due to underlying disease. If a patient had not relapsed or died at the time of data cutoff, duration of response was censored on the date for the last available visit. ‡Received a hematopoietic stem cell transplantation 30 days after CAR-T infusion. PR, partial remission. CR, complete remission. §Ongoing clinical responses.

even under conditions of prolonged antigen exposure. Consistent with the enhanced tumor killing ability, the cytotoxic effector molecules interferon-γ (IFN-γ), IL-2, and granzyme B were also increased in 20BBZ-OX40 CAR-T cells (Fig. 3, C to E). The expression of TNF-α varied in CAR-T cells from different donors. In two of three donors assessed, secreted TNF-α increased in 20BBZ-OX40 CAR-T cells, whereas it decreased in the other donor (fig. S13). The expression of IL-6 was slightly decreased in 20BBZ-OX40 CAR-T cells (fig. S13).

To test whether constitutive expression of OX40 affects the specificity of 20BBZ CAR-T cell cytotoxicity, we compared the cytotoxicity of 20BBZ-OX40 and 20BBZ CAR-T cells against $CD20^+$ and $CD20^-$

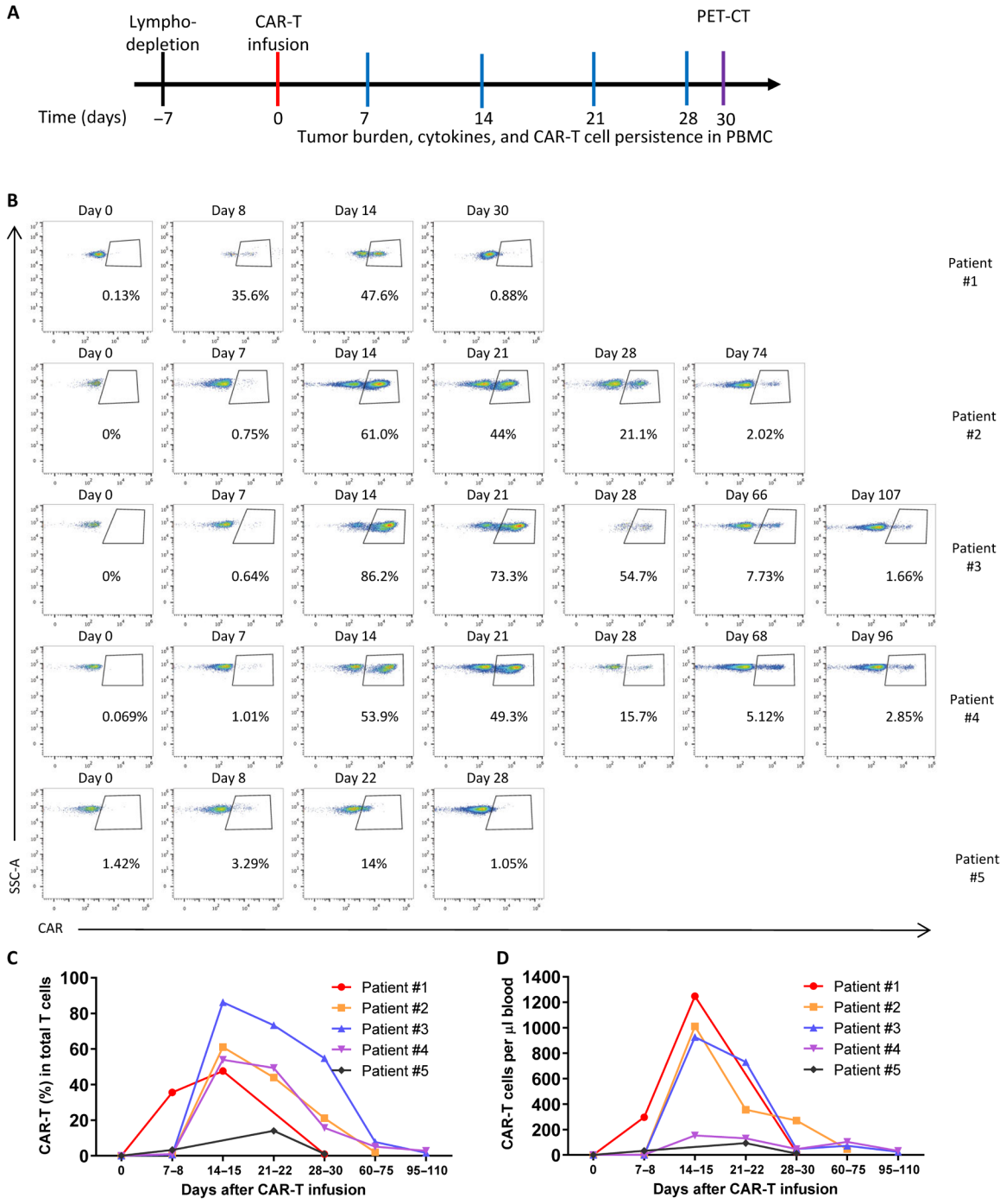

Fig. 5. Robust proliferation and persistence of 20BBZ-OX40 CAR-T cell in patients. (**A**) Schematic diagram of the clinical 20BBZ-OX40 CAR-T treatment regimen and sample analysis. (**B** and **C**) Flow cytometry analysis (B) and quantification (C) of the percentage of 20BBZ-OX40 CAR-T cells ($hCD45^+hCD19^-hCD3^+CAR^+$) in the $CD3^+$ T cell population from peripheral blood of patients at the indicated time points. (**D**) Absolute 20BBZ-OX40 CAR-T cell numbers in peripheral blood of patients at the indicated time points.

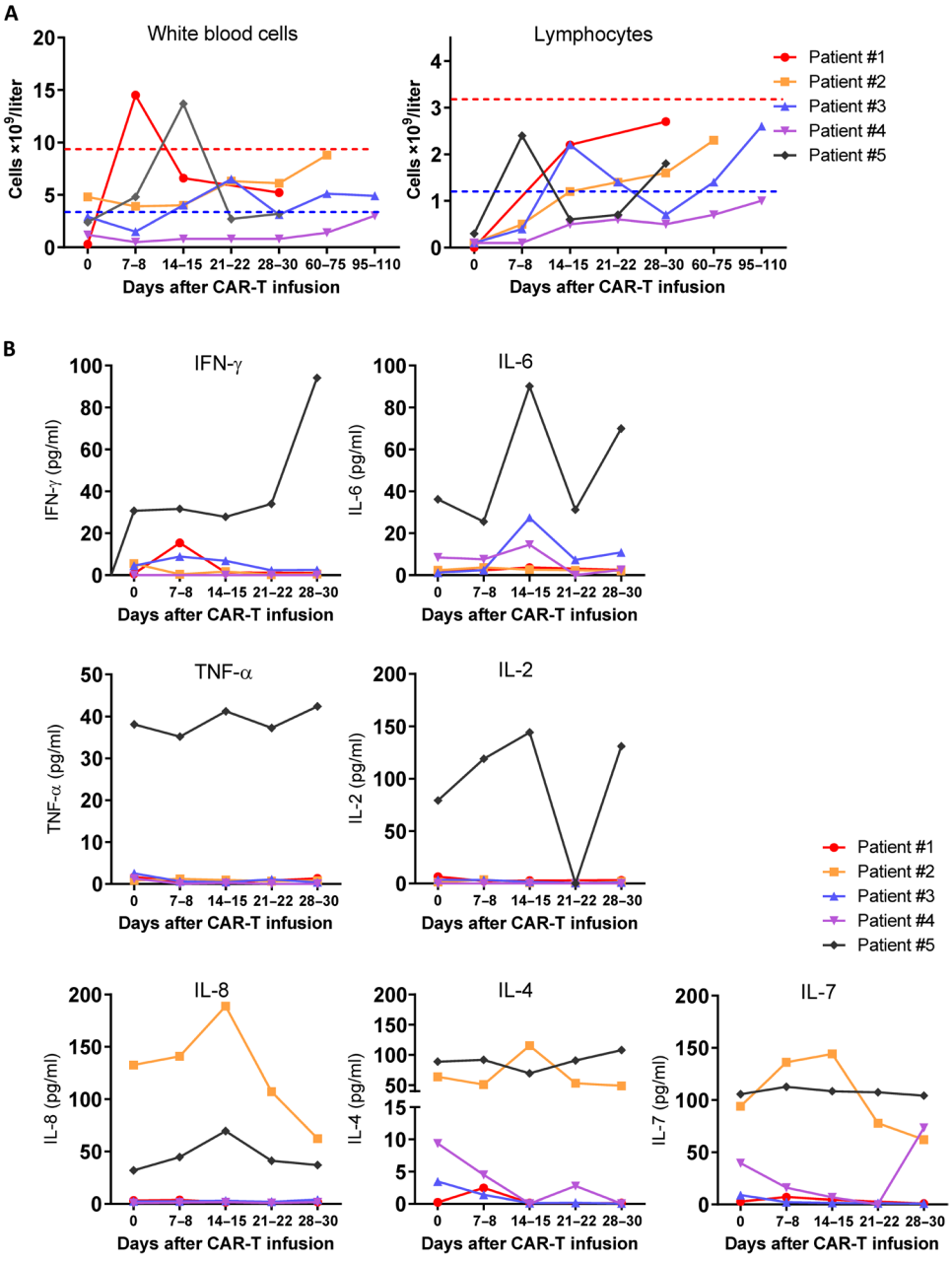

Fig. 6. Cytokine release profile after 20BBZ-OX40 CAR-T cell infusion. (**A**) White blood cell and lymphocyte counts from the peripheral blood of patients at the indicated time points. Red and blue dashed lines indicate the upper and lower boundaries of normal numbers of cells. (**B**) Cytokine concentrations in the serum of all patients who received infusions of 20BBZ-OX40 CAR-T cells, as determined by CBA assay.

tumor cells. 20BBZ-OX40 CAR-T cells showed stronger cytotoxicity than 20BBZ cells against $CD20^+$ target cells and were similarly ineffective at killing $CD20^-$ target cells (Fig. 3F). It is intriguing that 20BBZ-OX40 CAR-T cells had enhanced cytotoxicity for Nalm-6 cells expressing human CD20, because these cells have limited OX40L (fig. S1). This suggested that either constitutively expressed OX40 has some intrinsic, ligand-independent activity or even low amounts of OX40L are sufficient to initiate costimulatory signaling. Furthermore, these results suggested that OX40 provided a supportive costimulatory signal that enhanced CAR function but did not impair the specificity of CAR-T cells, which is similar to its natural role in TCR signaling.

20BBZ-OX40 CAR-T cells have improved persistence and antileukemia and antilymphoma effects in vivo

To determine whether the enhanced proliferation and cytotoxicity that we observed in culture with 20BBZ-OX40 CAR-T cells correlated with antitumor efficacy in vivo, we established a Raji xenograft tumor model in NSG mice. Seven days after intravenous inoculation with Raji cells, the NSG mice received intravenous injection of phosphate-buffered saline (PBS; control), 20BBZ CAR-T cells, or 20BBZ-OX40 CAR-T cells. CAR-T cell persistence and tumor cell burden in peripheral blood, spleen, and bone marrow were compared 7 days after infusion (Fig. 4, A to C). Consistent with the enhanced proliferation and cytotoxicity observed in vitro, a greater proportion of 20BBZ-OX40 CAR-T cells were present in bone marrow and peripheral blood mononuclear cells (PBMCs) compared with proportion of 20BBZ CAR-T cells (Fig. 4, A and C). Moreover, tumor burden in mice treated with 20BBZ-OX40 CAR-T cells was significantly lower than in those treated with 20BBZ CAR-T cells ($P < 0.05$; Fig. 4, A and C), indicating a stronger cytotoxic effect of 20BBZ-OX40 CAR-T cells than of 20BBZ CAR-T cells. We further tested the cytotoxicity of these CAR-T cells in an ex vivo killing assay. Bone marrow cells from CAR-T cell–treated mice were cocultured with Raji cells. Bone marrow cells from 20BBZ-OX40 CAR-T cell–treated mice eliminated most Raji tumor cells, whereas bone marrow cells from 20BBZ CAR-T cell–treated mice showed minimal cytotoxicity ($P < 0.001$; Fig. 4D).

The enhanced proliferation and cytotoxicity correlated with prolonged overall survival of 20BBZ-OX40 CAR-T cell–treated Raji tumor-bearing mice compared to the survival of the 20BBZ CAR-T cell treatment group ($P < 0.01$; Fig. 4E). We also evaluated the antitumor efficacy of 20BBZ-OX40 CAR-T cells on a B cell–derived Daudi tumor model. Daudi cells have abundant OX40L (fig. S1). As expected, enhanced tumor control was observed in mice receiving 20BBZ-OX40 CAR-T cells compared to mice receiving 20BBZ CAR-T cells ($P < 0.01$; Fig. 4F). These results suggested that 20BBZ-OX40 CAR-T cells persisted and proliferated in vivo and exhibited enhanced cytotoxicity ability compared with 20BBZ CAR-T cells in vivo.

Autologous 20BBZ-OX40 CAR-T therapy exhibited good tolerability and efficacy in patients with B cell lymphoma

To explore the safety and efficacy of 20BBZ-OX40 CAR-T cells as an anticancer treatment, we conducted a pilot study in patients with metastatic B cell lymphoma (table S2 and patient details are in the Supplementary Materials). We characterized the CD20BBZ-OX40 CAR-T cells before infusion (Table 1). The patients were all suffering from refractory and relapsed B cell lymphoma. Most B cell lymphomas are both $CD20^+$ and $CD19^+$. A total of five patients were enrolled, and all completed the 20BBZ-OX40 CAR-T cell treatment. Patient #1 received a hematopoietic stem cell transplantation 1 month after CAR-T cell infusion; therefore, this patient was excluded for evaluating the antitumor effect of CAR-T cell infusion. Seven days before CAR-T cell infusion, the patients received fludarabine (total dose of 30 mg/m^2 × 3) and cyclophosphamide (total dose of 750 mg/m^2 × 1) as a lympho-depleting preconditional treatment,

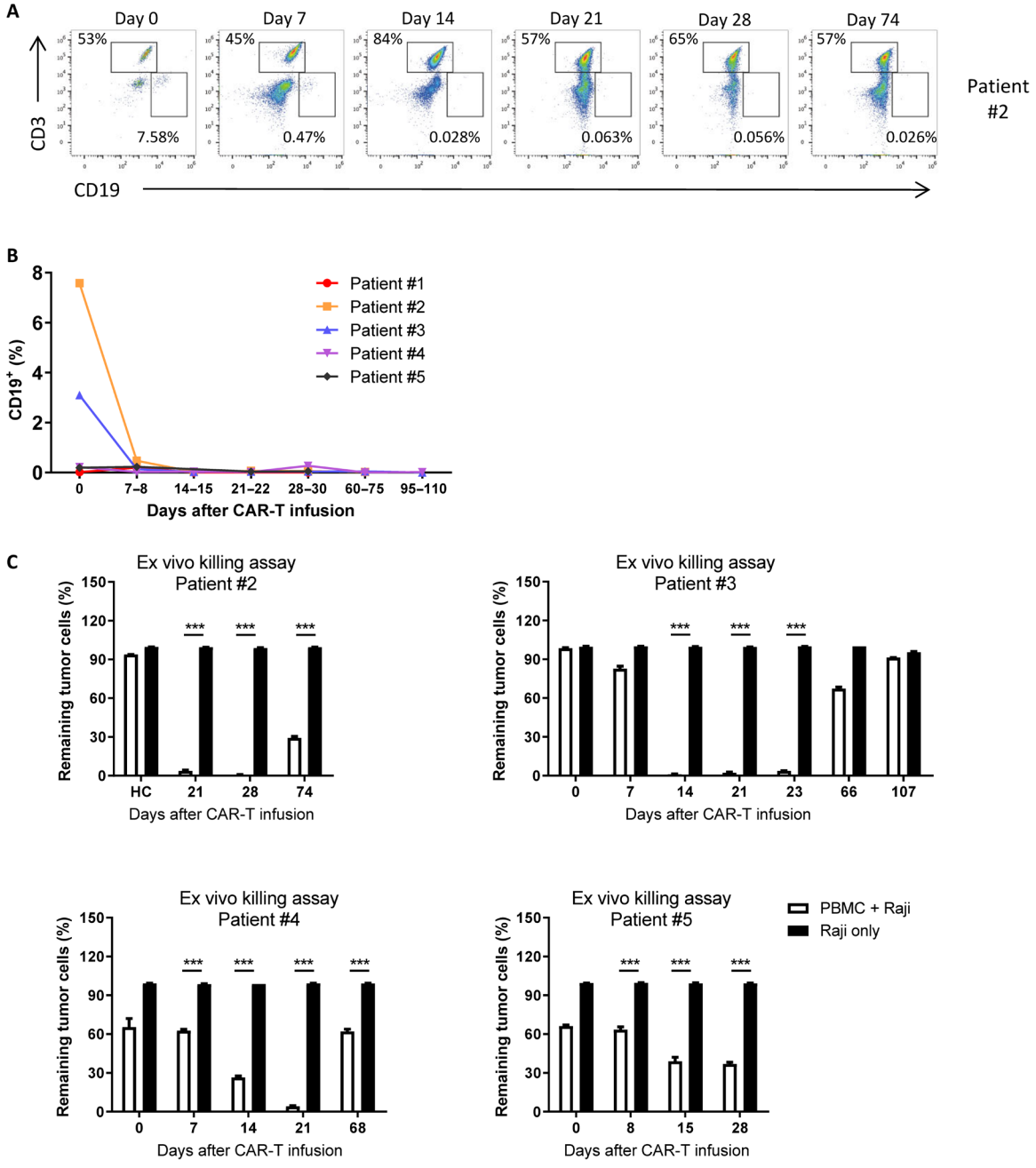

Fig. 7. Antitumor activity of 20BBZ-OX40 CAR-T cell in patients. (**A** and **B**) Flow cytometry analysis of the percentage of tumor or B cells ($hCD45^+hCD3^-hCD19^+$) and T cells ($hCD45^+hCD19^-hCD3^+$) in the peripheral blood from patient #2 (A) and summary of all patients (B). (**C**) At the indicated time point, PBMCs from the indicated patients were cocultured with Raji tumor cells ex vivo. Two days after coculture, tumor cells ($hCD14^-hCD56^-hCD3^-hCD19^+$) were analyzed by flow cytometry to assess ex vivo killing. Percentage of Raji cells remaining are shown as means ± SEM with statistical significance determined by unpaired *t* test (***$P < 0.001$). The normality of data was confirmed by Shapiro-Wilk test. HC, healthy donor control.

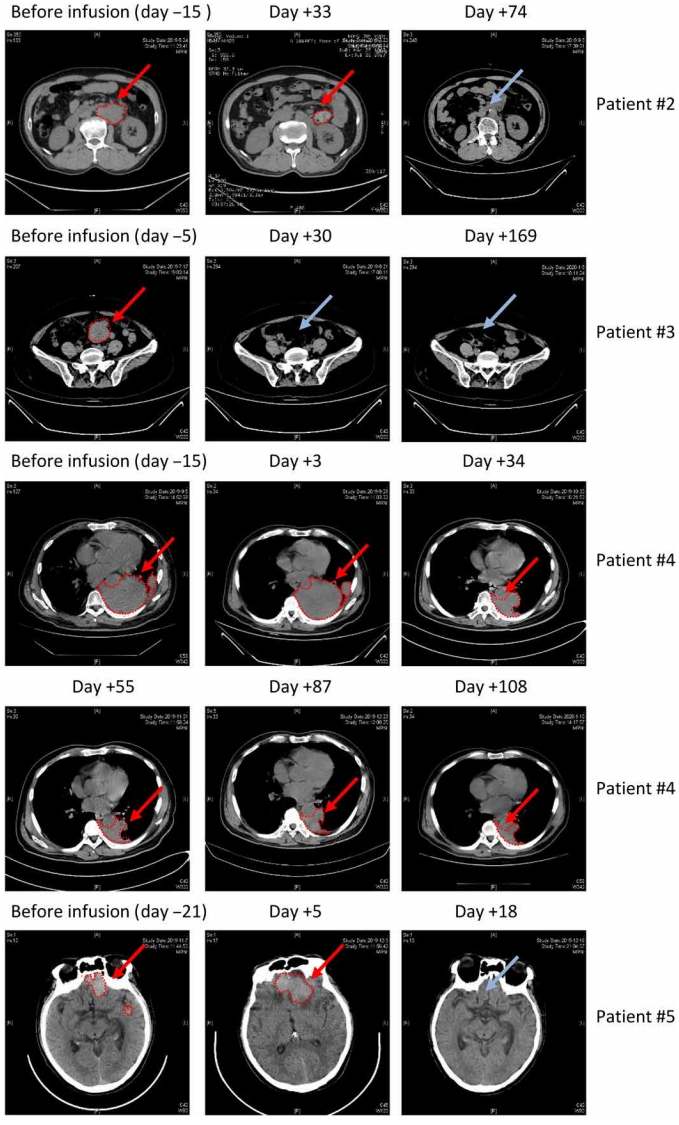

Fig. 8. Durable remission after 20BBZ-OX40 CAR-T cell treatment in patients. Representative PET-CT scans of patients #2, #4, and #5 and CT scans of patient #3 before and after 20BBZ-OX40 CAR-T cell treatment at the indicated time points. Lymphoma sites are indicated by red arrows and outlined with dotted lines. Light blue arrows indicate tumor reduction to undetectable. Patients #2 and #5 achieved complete remission, and patients #3 and #4 achieved partial remission.

and then a single dose of 20BBZ-OX40 CAR-T cells (1×10^6 to 4×10^6 cells/kg) was administered by infusion (Fig. 5A). CAR-T cell persistence and $CD19^+$ B cells were monitored on a weekly basis by flow cytometry using peripheral blood samples. In the peripheral blood, the proportion of CAR-T cells increased 7 to 28 days after infusion, indicating proliferation of these cells (Fig. 5, B to D). Previous clinical reports indicated that the CAR-T cells were about 3 to 25% of the total $CD3^+$ T cells at peak proliferation in patients with lymphoma (*43*). In our trial, in four of the five patients, 47 to 86% of $CD3^+$ T cells were 20BBZ-OX40 CAR-T cells at day 14, and the percentage of CAR-T cells was maintained at more than ~20% for the following 2 weeks (Fig. 5, B and C). For patients #1, #2, and #3, the CAR-T cell number at the peak increased more than 100-fold in circulation compared to the original infused cell number, which indicated strong proliferation of the original cell population (Fig. 5D).

Despite robust T cell proliferation, we did not observe severe side effects in any of the patients. The white blood cell and lymphocyte count was back to normal ranges about 1 month after CAR-T cell treatment for most patients (Fig. 6A). Furthermore, there was no CAR-T treatment–related severe cytokine release syndrome (CRS) over grade 1 (Fig. 6B) and no serious neurotoxicity (Table 1). These clinical results suggested that this type of CAR-T cell could have limited side effects despite the ability of this population of cells to robustly expand in vivo.

We analyzed whether 20BBZ-OX40 CAR-T cells had antitumor activity by monitoring normal B cells and B cell lymphoma cells in peripheral blood of patients. It is possible that CD20 is down-regulated after engaging 20BBZ-OX40 CAR-T cell, so we used CD19 as a marker for both normal B cells and lymphoma cells. After CAR-T cell treatment, $CD19^+$ cells were absent in the peripheral blood of all patients, which suggested CD20-targeted antitumor efficacy (Fig. 7, A and B, and fig. S14). Consistent with reduced B cells, serum immunoglobulin G (IgG) and IgM concentrations showed a declining trend for some patients during the monitored period (fig. S15). To test whether 20BBZ-OX40 CAR-T cells maintained their cytotoxicity, patient PBMCs were collected at different time points and cocultured with Raji tumor cells ex vivo. From days 14 to 107 after infusion, all PBMCs showed effective antitumor activity, whereas PBMCs collected before infusion or from healthy donor control had weak tumor killing ability (Fig. 7C). In four patients, metastatic tumors were substantially reduced after CAR-T cell infusion (Fig. 8). Among the five patients, two patients achieved complete remission, and three achieved partial remission after CAR-T cell treatment (Table 1). The objective response rate was 100%.

This pilot case study demonstrated that our 20BBZ-OX40 CAR-T cells are well tolerated in patients and have robust antitumor activity. Further investigation with a larger group of patients is needed to characterize these 20BBZ-OX40 CAR-T cells.

DISCUSSION

Despite superior antileukemia activity of CAR-T cells targeting CD19 in clinical trials, the efficacy of CAR-T cells in lymphoma or solid tumors is limited. To broaden the clinical usage and improve efficacy of CAR-T cells, an improved CAR-T cell construct is urgently needed. In this study, we generated an OX40-containing CAR-T cell against CD20 with enhanced in vivo and in vitro antitumor activity. Our results demonstrated that a separate and independently stimulated, rather than a CAR-integrated and antigen-stimulated, costimulatory OX40 signal is critical for sustaining the long-term activity of CAR-T cells. Compared with the widely used second generation of CAR-T cells, this approach has several advantages: (i) Constitutive signaling through OX40 induced by the tumor cells enhanced CAR-T cell proliferation and cytotoxicity after multiple exposures to antigen; (ii) the OX40 signal improved the antitumor activity and reduced the exhaustion of CAR-T cells; (iii) the OX40 signal improved the in vivo persistence, proliferation, and tumor killing ability of CAR-T cells; and (iv) the CAR-T cells with constitutively expressed OX40 were effective and safe in clinical settings.

Our CAR construct includes a separate constitutive costimulatory receptor that is not integrated into the CAR polypeptide. This construct had several advantages compared to current second- and third-generation CAR-T cell designs. The constitutively produced OX40 provides costimulatory signals that only modify the CAR-T cells without affecting bystander immune cells. This avoids potential mechanisms of toxicity associated with cytokine-secretion strategies (for example, IL-12 or IL-7) (*10*, *44*) or membrane-expressed immune-activating ligands (for example, 4-1BBL or CD40L) (*45*, *46*). Agonistic antibodies against the TNFR family (for example, antibodies activating CD40, 4-1BB, or OX40) induce moderate to severe liver toxicity (*47*). Forced constitutive expression of costimulatory ligands on CAR-T cells would function similarly to agonistic antibodies; therefore, this approach may cause similar adverse effects in clinical settings. However, our data showed that enhancing the costimulatory signal by constitutively expressing full-length OX40 may avoid this potential side effect. Similarly, a clinical trial using CAR-T cells with induced IL-12 secretion was halted after a correlation was demonstrated between serum IL-12 escalation and the manifestation of adverse effects (*48*). T cell survival–related cytokines, such as IL-7 and IL-15, were used to enhance the persistence of CAR-T cells (*10*, *14*). However, these strategies will increase the systemic amounts of these prosurvival cytokines. Thus, there is potential risk of leukemia after long-term exposure.

OX40 is produced as a separate protein from the CAR. This design can transduce OX40 signal upon OX40L engagement independent of the CAR-antigen interaction. During natural T cell activation, multiple costimulatory receptors are induced in a time-dependent fashion (*15*), which provide comprehensive and sustainable costimulatory signals for T cell activation and survival (*15*). Therefore, through the natural induction of additional costimulatory receptors or the activation of other naturally present costimulatory receptors, these OX40-expressing CAR-T cells can obtain additional costimulatory signals, which may contribute to their enhanced persistence in vivo.

The OX40 signal is ligand dependent. OX40L is found on activated B and T lymphocytes as well as myeloid-derived cells (*49*–*51*). These cell types are present in an immune-activated environment, which can be triggered by the initial CAR-T cell killing process. This immune-activated environment can provide positive feedback to enhance the function of CAR-T cells. Normal B cells and some B cell–derived lymphoblastic cell lines are positive for OX40L (*52*–*54*), which provides a specific activation niche for OX40-expressing CAR-T cells against B cell–derived tumors.

The OX40 signal promoted the survival of CAR-T cells during repeated tumor cell challenges. Our analysis revealed that the expression of multiple antiapoptotic genes was increased and that of proapoptotic genes was reduced. This suggested that the OX40 signal exerts a broad antiapoptotic influence within CAR-T cells that decreases their susceptibility to activation-induced cell death (AICD). Other approaches, such as constitutive IL7R activation or integrated signal transducer and activator of transcription 3 signaling or IL-15 signaling, also showed enhanced antiapoptotic characteristics (*14*, *55*, *56*). These CAR-T cell designs also have better persistence and antitumor efficacy both in vitro and in vivo (*14*, *55*, *56*). Reducing apoptosis appears to be an effective strategy for enhancing CAR-T cell persistence. T cells from mice lacking the gene encoding Fas, a death-inducing receptor, exhibit CAR-T cell survival under conditions of AICD (*57*). T cells from transgenic mice constitutively expressing Bcl-xL have better survival and less evidence of apoptosis compared to T cells from wild-type mice (*58*). It would be interesting to investigate whether the persistence of CAR-T cells could be improved by directly promoting antiapoptotic gene expression.

Among all these costimulatory receptors, OX40 was selected and enriched after multiple rounds of antigen stimulation in our screening system. Although all the TNFR family costimulatory receptors function similarly by recruiting TRAFs and activating NF-κB and MAPK pathways, each individual receptor is distinguished from the others by different TRAF recruitment, activation strength, and downstream signals (*17*). In addition, during T cell activation, these costimulatory receptors function at different stages of T cell activation and differentiation (*15*). OX40 recruits TRAF2, TRAF3, or TRAF5 and activates the NF-κB pathway (*21*, *26*, *27*). OX40 is induced later than CD28 and TNFR2, providing signals that promote continued division and survival when antigens are cleared (*21*). At a molecular level, OX40 signaling can activate the PI3K-AKT pathway and, in turn, promote expression of genes in the antiapoptotic BCL-2 family (*28*). Future investigation into the unique features of the OX40 pathway—including adaptor molecule recruitment, activation strength, signal duration, and key downstream effector molecules—is warranted. Quantifying these factors could further provide optimization strategies for improved CAR-T cell design.

Synergistic effects between 4-1BB and OX40 signaling in T cell effector function have been reported (*59*–*61*). In our model, we observed that OX40 enhanced BBZ-based CAR-T function but not 28Z-based CAR-T function. Thus, the enhancement that we observed with full-length OX40 and the 4-1BB signaling domain is consistent with previous findings in unmodified T cells (*59*–*61*). To further optimize CAR designs, evaluation of other potentially synergistic costimulation pairs is needed.

Limitations of our study include its small sample size and lack of a 20BBZ control group in the clinical trial. Although 20BBZ-OX40 CAR-T cells showed increased proliferation and cytotoxicity ability than 20BBZ CAR-T cells in vitro and in xenograft mouse models, a larger, multicenter, two-arm clinical trial is necessary to validate these findings in patients. Furthermore, our models are limited to leukemia and lymphoma and do not account for solid tumors. A solid tumor can generate an immune suppressive microenvironment at a cellular and a molecular level. It is unclear whether our approach could overcome the suppressive environment in solid tumors. In addition, most solid tumor targets for CAR-T therapy are tumor-associated antigens, and it is possible that our OX40-incorporated CAR design increases the risk of on-target but off-tumor adverse effects. Further investigation with solid tumor–targeting CARs will help to clarify these points. It would also be interesting to test whether OX40-incorporated CAR-T cells could be used as a component of a combination treatment against solid tumors.

In summary, we have developed a CAR construct with constitutive costimulatory receptor OX40 expression. This strategy equipped the T cells with distinct functional properties, including superior proliferative capacity and effector functions compared to the BBZ CAR-T cells that are widely used as a clinical therapeutic treatment. These characteristics lead to enhanced antitumor efficacy in various tumor models for leukemia and lymphoma in preclinical mouse models and clinical settings. Our CAR design could be used in other CAR-T cells, independent of antigen specificity, to enhance their antitumor efficacy and provides an alternative approach for improving the efficacy of CAR-T cells.

MATERIALS AND METHODS

Study design

The aim of this study was to identify potential CAR-T treatments with enhanced antitumor activity by integrating full-length costimulation receptors to the second generation of CAR. We established 12 CD20-targeting CAR-T cells with different costimulation receptors. By comparison of in vitro proliferation ability, we identified 20BBZ-OX40 as a candidate. We further investigated the signal transduction, antiapoptotic features, and cytotoxic ability of 20BBZ and 20BBZ-OX40 in vitro; antitumor activity in xenograft mice models; and safety and efficacy in a pilot investigator-initiated clinical trial. Investigators were not blinded to the experiments. The number of biological replicates and experiment replicates is described in each figure legend. Sample size was determined by previous experimental experience. In the xenograft models, mice were randomized into treatment groups.

A phase 1, single-center, open-label, and single-arm clinical trial was designed to evaluate the safety and feasibility of using autologous CD20BBZ-OX40 CAR-T cells (1×10^6 to 4×10^6 cells/kg of body weight) in patients with relapsed or refractory B cell lymphoma. The clinical protocol was reviewed and approved by the Medical Ethics Committee of The Affiliated Hospital of Xuzhou Medical University and has been registered at ClinicalTrials.gov with identifier number NCT03576807. The inclusion and exclusion criteria were listed in ClincalTrails.gov. Written informed consent was obtained from patients after potential risks were discussed. The patients received fludarabine (total dose of 30 mg/m^2 × 3) and cyclophosphamide (total dose of 750 mg/m^2 × 1) as a lympho-depleting preconditional treatment. Subsequently, a single dose of 20BBZ-OX40 CAR-T cells (1×10^6 to 4×10^6 cells/kg) was administered by infusion 5 days after lympho-depleting treatment. CRS was assessed and graded according to the CRS grading system developed by Lee *et al.* (*62*).

Mice

NOD-Prkdc^{scid}IL2rγ^{tm1} mice were purchased from Biocytogen Inc. or Shanghai Model Organisms Center Inc. All mice were maintained under specific pathogen–free conditions. Animal care and use were in accordance with institutional and National Institutes of Health protocols and guidelines, and all studies were approved by the Animal Care and Use Committee of Shanghai Jiao Tong University.

Cell lines and culture conditions

Lenti-X 293 was purchased from Clontech. Nalm-6 cell line was obtained from the American Type Culture Collection. Raji and Daudi cells were provided by the Stem Cell Bank, Chinese Academy of Sciences. Human PBMCs from cord blood were provided by Shanghai Longyao Biotechnology Limited. Informed written consent was obtained from all study participants, and the protocol was approved by the Suqian Obstetrics and Gynecology Hospital Ethics Committee and The Affiliated Hospital of Xuzhou Medical University. Nalm-6 cells were transduced with lentivirus that expressed hCD20. After selection with puromycin, resistant cells were subcloned, and hCD20-expressing cell lines were identified by anti-hCD20 flow cytometry analysis. Raji cells were transduced with hOX40L-expressing lentivirus. After puromycin selection, resistant cells were identified by anti-hOX40L flow cytometric analysis. Lenti-X 293 cells were cultured in Dulbecco's modified Eagle's medium supplemented with 9% heat-inactivated fetal bovine serum (FBS) (Gibco), 2 mM L-glutamine, 55 μM β-mercaptoethanol, penicillin (100 U/ml), and streptomycin (100 μg/ml). Raji, Nalm-6, Daudi, and human primary T cells were cultured in RPMI 1640 containing 9% heat-inactivated FBS, 2 mM L-glutamine, 55 μM β-mercaptoethanol, penicillin (100 U/ml), and streptomycin (100 μg/ml). All cells were cultured in a humidified incubator at 37°C supplemented with 5% CO_2.

Generation of lentiviral vectors

Lentiviral plasmids containing CAR constructs were generated by standard molecular cloning methods. Briefly, a DNA fragment containing the scFv recognizing human CD20 from rituximab, CD8 hinge and transmembrane domain, 4-1BB and CD3ζ intracellular domain, P2A sequences, and Bsi WI and Sal I restriction endonuclease sites was generated by overlap polymerase chain reaction (PCR) and subcloned into a modified pCDH-EF1a vector. The complementary DNA (cDNA) of individual costimulatory receptors was synthesized by Genewiz with 5′ Bsi WI and 3′ Sal I restriction endonuclease sites and subcloned into the intermediate CAR-containing plasmid. The amino acid sequences of 20BBZ and 20BBZ-OX40 are shown in table S1. The cDNA of human *CD20* or *OX40L* was PCR-amplified and subcloned into pCDH-EF1a-IRES-Puro using Eco RI and Bam HI sites to generate an *hCD20*-expressing plasmid.

Lentivirus production and transduction

Lentivirus was produced by transient transfection of Lenti-X 293 with a four-plasmid system. Supernatants containing lentivirus particles were collected 48 and 72 hours after transfection and concentrated by ultracentrifugation. Viral titer in transduction units per milliliter was determined by flow cytometry analysis of transduced Lenti-X 293 cells.

Transduction of human T cells

Human PBMCs from healthy donor umbilical cord blood were isolated with human PBMC separation fluid (Tbd Science). Total T cells were purified with the EasySep Human T Cell Isolation Kit (STEMCELL). T cells were cultured in RPMI 1640 complete medium supplemented with recombinant human (rh) IL-2 (50 IU/ml) and rhIL-21 (4 ng/ml). Plate-bound antibodies recognizing CD3 and soluble antibodies recognizing CD28 were used to activate T cells in culture. Two days after activation, various amounts of CAR-containing lentiviruses were used to transduce T cells at a multiplicity of infection of 10.

Repetitive stimulation assay

Lentivirus-transduced T cells were cultured with RPMI 1640 complete medium supplemented with rhIL-2 (50 IU/ml) and rhIL-21 (4 ng/ml). Irradiated (100-gray) Raji cells were used to stimulate these CAR-T cells at a ratio of 3:1 (T cells:Raji cells) first on day 6 after viral transduction and then once every 6 days during the entire culture period. The transduced T cells were maintained at a density of 1×10^6 to 2×10^6 cells/ml. Cells were monitored daily and fed according to cell counts every 1 to 2 days for a period of 22 to 25 days before use in vitro or in vivo experiments. On day 4 after indicated irradiated Raji cell stimulation round, the CAR-T cells were used for cytotoxicity assay, apoptosis and exhaustion marker analysis, and T cell subtype analysis.

Flow cytometry

For cell surface staining, cells were resuspended in staining buffer (1× PBS with 1% FBS) with antibodies recognizing CD16 and CD32

(anti-FcγRII and FcγRIII, clone 2.4 G2) or Human TruStain FcX (BioLegend) for 10 min to block nonspecific Fc-mediated binding. Blocked samples were subsequently stained with conjugated antibodies. Intracellular staining was performed after fixation for 30 min at room temperature in 4% paraformaldehyde and permeabilization with 1× Perm/Wash buffer (eBioscience) for 60 min at 4°C. Cells were incubated with indicated antibodies diluted in 1× Perm/Wash buffer for 30 min at 4°C. Annexin V staining was conducted in 1× annexin V binding buffer (BD Biosciences). To detect OX40L, Raji, Nalm-6, Daudi, 20BBZ-CAR-T, and T cells were prepared as a single-cell suspension and incubated with a phycoerythrin-conjugated antibody recognizing OX40L (Ancell) for 30 min or with OX40-Fc (Sino Biological) at a concentration of 2 μg/ml for 30 min and incubated with anti–hFc-AF647 secondary antibody for 30 min (Jackson ImmunoResearch). Cells were analyzed by CytoFLEX S flow cytometry (Beckman Coulter), and data were analyzed with FlowJo software (Becton Dickinson).

The following fluorescently labeled monoclonal antibodies were used with indicated dilution factor: goat anti-mouse IgG, F(ab')2 fragment specific (1: 2500; Jackson ImmunoResearch), human CD3 (1:250; clone OKT3, BioLegend), CD4 (1:250; clone OKT4, BioLegend), CD8α (1:250; clone HIT8a, BioLegend), OX40 (1:250; clone ACT35, BioLegend), PD-1 (1:250; clone eBioJ105, eBioscience), TIM-3 (1:250; clone F35-2E2, eBioscience), LAG-3 (1:250; clone 3DS223H, eBioscience), annexin V (1:50; BD Biosciences), and 7-AAD (1:25; BD Biosciences). CCR7 (clone 3D12, BD Biosciences), CD45RO (1:250; clone UCHL1, BioLegend), CD45RA (1:250; clone HI100, BioLegend), CD45 (1:250; clone HI30, eBioscience), CD19 (1:250; clone HIB19, eBioscience), active caspase-3 (1:250; clone C92-605, BD Biosciences), IFN-γ (1:250; clone 4SB3, BioLegend), granzyme B (1:250; clone QA16A02, BioLegend), CD14 (1:250; clone HCD14, BioLegend), CD56 (1:250; clone HCD56, BioLegend), and mouse CD45 (1:250; clone 30-F11, BioLegend).

Western blot analysis

20BBZ or 20BBZ-OX40 CAR-T cells were stimulated with OX40L-overexpressing Raji-OX40L cell line for 15, 30, 60, and 120 min; harvested; and lysed with radioimmunoprecipitation assay lysis buffer (#9803, Cell Signaling Technology). Protein lysates were separated by SDS–polyacrylamide gel electrophoresis under reducing conditions. Immune blotting was carried out with the following antibodies: 1:5000 dilution anti–glyceraldehyde-3-phosphate dehydrogenase (GAPDH) (clone GAPDH-71.1, Sigma-Aldrich), 1:1000 dilution anti–phospho-p65 (#3030, Cell Signaling Technology), 1:1000 dilution anti–phospho-ERK (Thr^{202}/Tyr^{204}) (#4370, Cell Signaling Technology), 1:1000 dilution anti–phospho-AKT (Ser^{473}) (#4060, Cell Signaling Technology), 1:5000 dilution horseradish peroxidase (HRP)–conjugated anti-mouse IgG (H + L) (ZSGB-Bio), and 1:5000 dilution HRP-conjugated anti-rabbit IgG (H + L) (ZSGB-Bio). All images were acquired on a ChemiDoc MP system (Bio-Rad).

For experiments performed with small molecular inhibitors of PI3K (wortmannin), AKT (afuresertib), IκB kinase (IKK) (MLN120B or BMS-345541), and ERK1/2 (ravoxertinib, ulixertinib, cobimetinib, or trametinib), the inhibitors were purchased from MedChemExpress. 20BBZ-OX40 CAR-T cells were pretreated with the indicated small molecular inhibitors for 6 hours before stimulation with Raji-OX40L cells for 15 min. Cells were then harvested, lysed, and subjected to Western blotting for phospho-p65, phospho-ERK, and phospho-AKT.

CAR-T proliferation assay with small molecular inhibitors

20BBZ-OX40 CAR-T cells were stimulated with irradiated Raji cells once on day 0 in the presence of inhibitors of PI3K (wortmannin), AKT (afuresertib), IKK (MLN120B or BMS-345541), or ERK1/2 (cobimetinib or trametinib). The culture medium was refreshed with indicated inhibitors every 2 days. Four days later, CAR-T cell numbers were counted.

In vitro CAR-T cell cytotoxicity assay

For Raji and Nalm-6-hCD20 cells, a total of 1×10^5 CAR-T cells were cocultured with 1×10^5, 2×10^5, or 4×10^5 $CD20^+$ tumor cells in a flat-bottom 96-well plate. Twenty-four, 48, and 72 hours after plating, cells were harvested and analyzed by flow cytometry. Anti-CD3 and anti-CD19 were used to distinguish CAR-T and tumor cells, respectively.

Cytokine production analysis

Production of the cytokines IFN-γ, IL-2, IL-6, IL-8, IL-7, IL-4, and TNF-α in culture supernatants or plasma was quantified using Cytometric Bead Array (CBA) kits (BD Biosciences) according to the manufacturer's instructions.

Gene expression and CAR-T persistence analysis by quantitative PCR

Total RNA from CAR-T cells was extracted with the Total RNA Kit (Omega Bio-tek) and reverse-transcribed into cDNA with ReverTra Ace reverse transcriptase (Toyobo). Quantitative PCR reactions were performed in triplicate with SYBR Green Supermix (Toyobo). The relative quantification of the products was calculated by the 2-ΔΔCt method. The following specific primers were synthesized and obtained from Genewiz: hIFN-γ (forward), TCGGTAACTGACTTGAATGTCCA; hIFN-γ (reverse), TCGCTTCCCTGTTTTAGCTGC; hGAPDH (forward), GGAGCGAGATCCCTCCAAAAT; hGAPDH (reverse), GGCTGTTGTCATACTTCTCATGG; hSurvivin (forward), AGGACCACCGCATCTCTACAT; hSurvivin (reverse), AAGTCTGGCTCGTTCTCAGTG; hGZMB (forward), TACCATTGAGTTGTGCGTGGG; hGZMB (reverse), GCCATTGTTTCGTCCATAGGAGA; hBcl-2 (forward), GGTGGGGTCATGTGTGTGG; hBcl-2 (reverse), CGGTTCAGGTACTCAGTCATCC; hBcl-xl (forward), GAGCTGGTGGTTGACTTTCTC; hBcl-xl (reverse), TCCATCTCCGATTCAGTCCCT; hBax (forward), CCCGAGAGGTCTTTTTCCGAG; hBax (reverse), CCAGCCCATGATGGTTCTGAT.

Animal models

To evaluate the antitumor activity of CD20-targeted CAR-T cells against leukemia or lymphoma, female NOD-$Prkdc^{scid}IL2r\gamma^{tm1}$ mice were inoculated with 1×10^6 Raji or Daudi cells intravenously. About 7 days later, 1×10^7 CAR-T cells or a PBS control was infused intravenously, and animal survival was monitored over time. To evaluate the tumor burden and CAR-T cell persistence in vivo, peripheral blood, spleens, and bone marrow from femurs and tibias were harvested, and single-cell suspensions were generated for flow cytometry analysis. Spleens were manually homogenized in PBS and passed through a 70-μm cell strainer (BD Biosciences). To obtain cells from bone marrow, the femurs and tibias were flushed with PBS using a 1-ml syringe (KDL). ACK (Ammonium-Chloride-Potassium) lysing buffer (BD Biosciences) was used to lyse red blood cells in all samples.

CAR-T cell manufacture for clinical usage

PBMCs were collected from patients by leukapheresis and purified by Ficoll-Paque density gradient centrifugation. T cells were enriched by CD4- and CD8-positive selection (Miltenyi Biotec) and were then stimulated with anti-CD3 and anti-CD28 beads. T cells were cultured in X-VIVO 15 medium supplemented with rhIL-2 and rhIL-21. Two days after T cell activation, cells were transduced with a lentivirus encoding 20BBZ-OX40 CAR. Cells were then grown for an additional 11 to 13 days and frozen in liquid nitrogen. Quality checks were performed during the CAR-T cell manufacturing process.

Statistics

Statistical analyses were performed using Prism 8 (GraphPad Software Inc). Significance of in vitro assays was determined by a two-sided Student's unpaired *t* test, Mann-Whitney *U* test, or one-way analysis of variance (ANOVA) with Dunnett's multiple comparisons correction. When unpaired *t* test was applied, the normality of data was confirmed by Shapiro-Wilk test with a *P* value of >0.05. A two-sided log-rank test was applied to assess mouse survival. Where indicated, $*P < 0.05$, $**P < 0.01$, and $***P < 0.001$ were considered statistically significant results.

SUPPLEMENTARY MATERIALS

stm.sciencemag.org/cgi/content/full/13/578/eaba7308/DC1

Patient details: Tumor burden, bridging chemotherapy, and toxicity management information.
Fig. S1. OX40L abundance on different types of cells.
Fig. S2. Profile of indicated small molecular inhibitors targeting ERK1/2, IKK, and PI3K/AKT.
Fig. S3. Small molecular inhibitors targeting ERK1/2, IKK, and PI3K/AKT inhibited the proliferation of CAR-T cells.
Fig. S4. Proliferation of 20BBZ-OX40 CAR-T cells.
Fig. S5. Proliferation of 20BBOXZ, 20OXBBZ, and 20BBZ-OX40 CAR-T cells.
Fig. S6. Proliferation of 20Z, 20Z-OX40, and 20BBZ CAR-T cells.
Fig. S7. Proliferation and cytotoxic ability of 19BBZ and 19BBZ-OX40 CAR-T cells.
Fig. S8. Proliferation of 1928Z and1928Z-OX40 CAR-T cells.
Fig. S9. 20BBZ-OX40 CAR-T cells are less apoptotic than 20BBZ CAR-T cells.
Fig. S10. T cell effector and memory subtype analysis of 20BBZ and 20BBZ-OX40 CAR-T cells.
Fig. S11. $CD4^+$ and $CD8^+$ T cell subtype analysis of 20BBZ and 20BBZ-OX40 CAR-T cells.
Fig. S12. Cytotoxicity of 20BBZ-OX40 CAR-T cells.
Fig. S13. Cytokine release from 20BBZ and 20BBZ-OX40 CAR-T cells.
Fig. S14. Characterization of the clinical efficacy profile of 20BBZ-OX40 CAR-T in patients.
Fig. S15. Immunoglobulin profile after 20BBZ-OX40 CAR-T cell infusion.
Table S1. Amino acid sequences of 20BBZ and 20BBZ-OX40.
Table S2. CAR-T cell characteristics before patient infusion.
Data file S1. Data file for all figures.

View/request a protocol for this paper from *Bio-protocol*.

REFERENCES AND NOTES

1. S. H. Baumeister, G. J. Freeman, G. Dranoff, A. H. Sharpe, Coinhibitory pathways in immunotherapy for cancer. *Annu. Rev. Immunol.* **34**, 539–573 (2016).
2. W. Zou, J. D. Wolchok, L. Chen, PD-L1 (B7-H1) and PD-1 pathway blockade for cancer therapy: Mechanisms, response biomarkers, and combinations. *Sci. Transl. Med.* **8**, 328rv324 (2016).
3. S. Guedan, M. Ruella, C. H. June, Emerging cellular therapies for cancer. *Annu. Rev. Immunol.* **37**, 145–171 (2019).
4. J. Tang, V. M. Hubbard-Lucey, L. Pearce, J. O'Donnell-Tormey, A. Shalabi, The global landscape of cancer cell therapy. *Nat. Rev. Drug Discov.* **17**, 465–466 (2018).
5. S. Gill, M. V. Maus, D. L. Porter, Chimeric antigen receptor T cell therapy: 25 years in the making. *Blood Rev.* **30**, 157–167 (2016).
6. W. A. Lim, C. H. June, The principles of engineering immune cells to treat cancer. *Cell* **168**, 724–740 (2017).
7. K. Watanabe, S. Kuramitsu, A. D. Posey Jr., C. H. June, Expanding the therapeutic window for CAR T cell therapy in solid tumors: The knowns and unknowns of CAR T cell biology. *Front. Immunol.* **9**, 2486 (2018).
8. R. S. Riley, C. H. June, R. Langer, M. J. Mitchell, Delivery technologies for cancer immunotherapy. *Nat. Rev. Drug Discov.* **18**, 175–196 (2019).
9. M. A. Morgan, A. Schambach, Engineering CAR-T cells for improved function against solid tumors. *Front. Immunol.* **9**, 2493 (2018).
10. K. Adachi, Y. Kano, T. Nagai, N. Okuyama, Y. Sakoda, K. Tamada, IL-7 and CCL19 expression in CAR-T cells improves immune cell infiltration and CAR-T cell survival in the tumor. *Nat. Biotechnol.* **36**, 346–351 (2018).
11. S. Sukumaran, N. Watanabe, P. Bajgain, K. Raja, S. Mohammed, W. E. Fisher, M. K. Brenner, A. M. Leen, J. F. Vera, Enhancing the potency and specificity of engineered T cells for cancer treatment. *Cancer Discov.* **8**, 972–987 (2018).
12. X. Liu, R. Ranganathan, S. Jiang, C. Fang, J. Sun, S. Kim, K. Newick, A. Lo, C. H. June, Y. Zhao, E. K. Moon, A chimeric switch-receptor targeting pd1 augments the efficacy of second-generation CAR T cells in advanced solid tumors. *Cancer Res.* **76**, 1578–1590 (2016).
13. S. Rafiq, O. O. Yeku, H. J. Jackson, T. J. Purdon, D. G. van Leeuwen, D. J. Drakes, M. Song, M. M. Miele, Z. Li, P. Wang, S. Yan, J. Xiang, X. Ma, V. E. Seshan, R. C. Hendrickson, C. Liu, R. J. Brentjens, Targeted delivery of a PD-1-blocking scFv by CAR-T cells enhances anti-tumor efficacy in vivo. *Nat. Biotechnol.* **36**, 847–856 (2018).
14. L. V. Hurton, H. Singh, A. M. Najjar, K. C. Switzer, T. Mi, S. Maiti, S. Olivares, B. Rabinovich, H. Huls, M. A. Forget, V. Datar, P. Kebriaei, D. A. Lee, R. E. Champlin, L. J. N. Cooper, Tethered IL-15 augments antitumor activity and promotes a stem-cell memory subset in tumor-specific T cells. *Proc. Natl. Acad. Sci. U.S.A.* **113**, E7788–E7797 (2016).
15. L. Chen, D. B. Flies, Molecular mechanisms of T cell co-stimulation and co-inhibition. *Nat. Rev. Immunol.* **13**, 227–242 (2013).
16. Q. Zhang, D. A. Vignali, Co-stimulatory and co-inhibitory pathways in autoimmunity. *Immunity* **44**, 1034–1051 (2016).
17. T. H. Watts, TNF/TNFR family members in costimulation of T cell responses. *Annu. Rev. Immunol.* **23**, 23–68 (2005).
18. R. M. Locksley, N. Killeen, M. J. Lenardo, The TNF and TNF receptor superfamilies: Integrating mammalian biology. *Cell* **104**, 487–501 (2001).
19. M. Croft, Co-stimulatory members of the TNFR family: Keys to effective T-cell immunity? *Nat. Rev. Immunol.* **3**, 609–620 (2003).
20. J. Willoughby, J. Griffiths, I. Tews, M. S. Cragg, OX40: Structure and function - What questions remain? *Mol. Immunol.* **83**, 13–22 (2017).
21. P. R. Rogers, J. Song, I. Gramaglia, N. Killeen, M. Croft, OX40 promotes Bcl-xL and Bcl-2 expression and is essential for long-term survival of CD4 T cells. *Immunity* **15**, 445–455 (2001).
22. S. Salek-Ardakani, J. Song, B. S. Halteman, A. G. H. Jember, H. Akiba, H. Yagita, M. Croft, OX40 (CD134) controls memory T helper 2 cells that drive lung inflammation. *J. Exp. Med.* **198**, 315–324 (2003).
23. T. So, J. Song, K. Sugie, A. Altman, M. Croft, Signals from OX40 regulate nuclear factor of activated T cells c1 and T cell helper 2 lineage commitment. *Proc. Natl. Acad. Sci. U.S.A.* **103**, 3740–3745 (2006).
24. J. Song, T. So, M. Cheng, X. Tang, M. Croft, Sustained survivin expression from OX40 costimulatory signals drives T cell clonal expansion. *Immunity* **22**, 621–631 (2005).
25. X. Xiao, S. Balasubramanian, W. Liu, X. Chu, H. Wang, E. J. Taparowsky, Y. X. Fu, Y. Choi, M. C. Walsh, X. C. Li, OX40 signaling favors the induction of T(H)9 cells and airway inflammation. *Nat. Immunol.* **13**, 981–990 (2012).
26. R. H. Arch, C. B. Thompson, 4-1BB and Ox40 are members of a tumor necrosis factor (TNF)-nerve growth factor receptor subfamily that bind TNF receptor-associated factors and activate nuclear factor kappaB. *Mol. Cell. Biol.* **18**, 558–565 (1998).
27. S. Kawamata, T. Hori, A. Imura, A. Takaori-Kondo, T. Uchiyama, Activation of OX40 signal transduction pathways leads to tumor necrosis factor receptor-associated factor (TRAF) 2- and TRAF5-mediated NF-κB activation. *J. Biol. Chem.* **273**, 5808–5814 (1998).
28. T. So, H. Choi, M. Croft, OX40 complexes with phosphoinositide 3-kinase and protein kinase B (PKB) to augment TCR-dependent PKB signaling. *J. Immunol.* **186**, 3547–3555 (2011).
29. T. So, M. Croft, Regulation of PI-3-kinase and Akt signaling in T lymphocytes and other cells by TNFR family molecules. *Front. Immunol.* **4**, 139 (2013).
30. J. Song, S. Salek-Ardakani, T. So, M. Croft, The kinases aurora B and mTOR regulate the G1–S cell cycle progression of T lymphocytes. *Nat. Immunol.* **8**, 64–73 (2007).
31. D. L. Porter, B. L. Levine, M. Kalos, A. Bagg, C. H. June, Chimeric antigen receptor-modified T cells in chronic lymphoid leukemia. *N. Engl. J. Med.* **365**, 725–733 (2011).
32. A. A. Shaimardanova, K. V. Kitaeva, I. I. Abdrakhmanova, V. M. Chernov, C. S. Rutland, A. A. Rizvanov, D. S. Chulpanova, V. V. Solovyeva, Production and application of multicistronic constructs for various human disease therapies. *Pharmaceutics* **11**, 580 (2019).
33. M. Croft, T. So, W. Duan, P. Soroosh, The significance of OX40 and OX40L to T-cell biology and immune disease. *Immunol. Rev.* **229**, 173–191 (2009).
34. R. Arafeh, K. Flores, A. Keren-Paz, G. Maik-Rachline, N. Gutkind, S. Rosenberg, R. Seger, Y. Samuels, Combined inhibition of MEK and nuclear ERK translocation has synergistic antitumor activity in melanoma cells. *Sci. Rep.* **7**, 16345 (2017).
35. C. Ning, M. Liang, S. Liu, G. Wang, H. Edwards, Y. Xia, L. Polin, G. Dyson, J. W. Taub, R. M. Mohammad, A. S. Azmi, L. Zhao, Y. Ge, Targeting ERK enhances the cytotoxic effect of the novel PI3K and mTOR dual inhibitor VS-5584 in preclinical models of pancreatic cancer. *Oncotarget* **8**, 44295–44311 (2017).

36. Y. Q. Li, Y. Zhong, X. P. Xiao, D. D. Li, Z. Zhou, Y. Y. Tian, IL-33/ST2 axis promotes the inflammatory response of nasal mucosal epithelial cells through inducing the ERK1/2 pathway. *Innate Immun.* **26**, 505–513 (2020).
37. M. Yamaji, A. Ota, M. Wahiduzzaman, S. Karnan, T. Hyodo, H. Konishi, S. Tsuzuki, Y. Hosokawa, M. Haniuda, Novel ATP-competitive Akt inhibitor afuresertib suppresses the proliferation of malignant pleural mesothelioma cells. *Cancer Med.* **6**, 2646–2659 (2017).
38. G. Manzella, L. D. Schreck, W. B. Breunis, J. Molenaar, H. Merks, F. G. Barr, W. Sun, M. Römmele, L. Zhang, J. Tchinda, Q. A. Ngo, P. Bode, O. Delattre, D. Surdez, B. Rekhi, F. K. Niggli, B. W. Schäfer, M. Wachtel, Phenotypic profiling with a living biobank of primary rhabdomyosarcoma unravels disease heterogeneity and AKT sensitivity. *Nat. Commun.* **11**, 4629 (2020).
39. J. Mookerjee Basu, A. Mookerjee, P. Sen, S. Bhaumik, P. Sen, S. Banerjee, K. Naskar, S. K. Choudhuri, B. Saha, S. Raha, S. Roy, Sodium antimony gluconate induces generation of reactive oxygen species and nitric oxide via phosphoinositide 3-kinase and mitogen-activated protein kinase activation in Leishmania donovani-infected macrophages. *Antimicrob. Agents Chemother.* **50**, 1788–1797 (2006).
40. N. Bernabo, M. Mattioli, B. Barboni, Signal transduction in the activation of spermatozoa compared to other signalling pathways: A biological networks study. *Int. J. Data Min. Bioinform.* **12**, 59–69 (2015).
41. A. D. Weinberg, M. M. Rivera, R. Prell, A. Morris, T. Ramstad, J. T. Vetto, W. J. Urba, G. Alvord, C. Bunce, J. Shields, Engagement of the OX-40 receptor in vivo enhances antitumor immunity. *J. Immunol.* **164**, 2160–2169 (2000).
42. S. Guedan, A. D. Posey Jr., C. Shaw, A. Wing, T. Da, P. R. Patel, S. E. McGettigan, V. Casado-Medrano, O. U. Kawalekar, M. Uribe-Herranz, D. Song, J. J. Melenhorst, S. F. Lacey, J. Scholler, B. Keith, R. M. Young, C. H. June, Enhancing CAR T cell persistence through ICOS and 4-1BB costimulation. *JCI Insight* **3**, e96976 (2018).
43. Z. Ying, X. F. Huang, X. Xiang, Y. Liu, X. Kang, Y. Song, X. Guo, H. Liu, N. Ding, T. Zhang, P. Duan, Y. Lin, W. Zheng, X. Wang, N. Lin, M. Tu, Y. Xie, C. Zhang, W. Liu, L. Deng, S. Gao, L. Ping, X. Wang, N. Zhou, J. Zhang, Y. Wang, S. Lin, M. Mamuti, X. Yu, L. Fang, S. Wang, H. Song, G. Wang, L. Jones, J. Zhu, S. Y. Chen, A safe and potent anti-CD19 CAR T cell therapy. *Nat. Med.* **25**, 947–953 (2019).
44. L. Zhang, R. A. Morgan, J. D. Beane, Z. Zheng, M. E. Dudley, S. H. Kassim, A. V. Nahvi, L. T. Ngo, R. M. Sherry, G. Q. Phan, M. S. Hughes, U. S. Kammula, S. A. Feldman, M. A. Toomey, S. P. Kerkar, N. P. Restifo, J. C. Yang, S. A. Rosenberg, Tumor-infiltrating lymphocytes genetically engineered with an inducible gene encoding interleukin-12 for the immunotherapy of metastatic melanoma. *Clin. Cancer Res.* **21**, 2278–2288 (2015).
45. Z. Zhao, M. Condomines, S. J. C. van der Stegen, F. Perna, C. C. Kloss, G. Gunset, J. Plotkin, M. Sadelain, Structural design of engineered costimulation determines tumor rejection kinetics and persistence of CAR T cells. *Cancer Cell* **28**, 415–428 (2015).
46. N. F. Kuhn, T. J. Purdon, D. G. van Leeuwen, A. V. Lopez, K. J. Curran, A. F. Daniyan, R. J. Brentjens, CD40 ligand-modified chimeric antigen receptor T cells enhance antitumor function by eliciting an endogenous antitumor response. *Cancer Cell* **35**, 473–488.e6 (2019).
47. X. Qi, F. Li, Y. Wu, C. Cheng, P. Han, J. Wang, X. Yang, Optimization of 4-1BB antibody for cancer immunotherapy by balancing agonistic strength with FcγR affinity. *Nat. Commun.* **10**, 2141 (2019).
48. H. J. Pegram, J. C. Lee, E. G. Hayman, G. H. Imperato, T. F. Tedder, M. Sadelain, R. J. Brentjens, Tumor-targeted T cells modified to secrete IL-12 eradicate systemic tumors without need for prior conditioning. *Blood* **119**, 4133–4141 (2012).
49. S. M. Jensen, L. D. Maston, M. J. Gough, C. E. Ruby, W. L. Redmond, M. Crittenden, Y. Li, S. Puri, C. H. Poehlein, N. Morris, M. Kovacsovics-Bankowski, T. Moudgil, C. Twitty, E. B. Walker, H. M. Hu, W. J. Urba, A. D. Weinberg, B. Curti, B. A. Fox, Signaling through OX40 enhances antitumor immunity. *Semin. Oncol.* **37**, 524–532 (2010).
50. K. Sugamura, N. Ishii, A. D. Weinberg, Therapeutic targeting of the effector T-cell co-stimulatory molecule OX40. *Nat. Rev. Immunol.* **4**, 420–431 (2004).
51. M. J. Gough, A. D. Weinberg, OX40 (CD134) and OX40L. *Adv. Exp. Med. Biol.* **647**, 94–107 (2009).
52. P. J. Linton, B. Bautista, E. Biederman, E. S. Bradley, J. Harbertson, R. M. Kondrack, R. C. Padrick, L. M. Bradley, Costimulation via OX40L expressed by B cells is sufficient to determine the extent of primary CD4 cell expansion and Th2 cytokine secretion in vivo. *J. Exp. Med.* **197**, 875–883 (2003).
53. A. Cortini, U. Ellinghaus, T. H. Malik, D. S. Cunninghame Graham, M. Botto, T. J. Vyse, B cell OX40L supports T follicular helper cell development and contributes to SLE pathogenesis. *Ann. Rheum. Dis.* **76**, 2095–2103 (2017).
54. D. Reuter, M. S. Staege, C. D. Kuhnöl, J. Föll, Immunostimulation by OX40 ligand transgenic Ewing sarcoma cells. *Front. Oncol.* **5**, 242 (2015).
55. Y. Kagoya, S. Tanaka, T. Guo, M. Anczurowski, C. H. Wang, K. Saso, M. O. Butler, M. D. Minden, N. Hirano, A novel chimeric antigen receptor containing a JAK-STAT signaling domain mediates superior antitumor effects. *Nat. Med.* **24**, 352–359 (2018).
56. T. Shum, B. Omer, H. Tashiro, R. L. Kruse, D. L. Wagner, K. Parikh, Z. Yi, T. Sauer, D. Liu, R. Parihar, P. Castillo, H. Liu, M. K. Brenner, L. S. Metelitsa, S. Gottschalk, C. M. Rooney, Constitutive signaling from an engineered IL7 receptor promotes durable tumor elimination by tumor-redirected T cells. *Cancer Discov.* **7**, 1238–1247 (2017).
57. J. Ren, X. Zhang, X. Liu, C. Fang, S. Jiang, C. H. June, Y. Zhao, A versatile system for rapid multiplex genome-edited CAR T cell generation. *Oncotarget* **8**, 17002–17011 (2017).
58. D. A. Grillot, R. Merino, G. Nunez, Bcl-XL displays restricted distribution during T cell development and inhibits multiple forms of apoptosis but not clonal deletion in transgenic mice. *J. Exp. Med.* **182**, 1973–1983 (1995).
59. A. Konstorum, A. T. Vella, A. J. Adler, R. C. Laubenbacher, A mathematical model of combined CD8 T cell costimulation by 4-1BB (CD137) and OX40 (CD134) receptors. *Sci. Rep.* **9**, 10862 (2019).
60. S. J. Lee, R. J. Rossi, S. K. Lee, M. Croft, B. S. Kwon, R. S. Mittler, A. T. Vella, CD134 costimulation couples the CD137 pathway to induce production of supereffector CD8 T cells that become IL-7 dependent. *J. Immunol.* **179**, 2203–2214 (2007).
61. S. J. Lee, L. Myers, G. Muralimohan, J. Dai, Y. Qiao, Z. Li, R. S. Mittler, A. T. Vella, 4-1BB and OX40 dual costimulation synergistically stimulate primary specific CD8 T cells for robust effector function. *J. Immunol.* **173**, 3002–3012 (2004).
62. D. W. Lee, R. Gardner, D. L. Porter, C. U. Louis, N. Ahmed, M. Jensen, S. A. Grupp, C. L. Mackall, Current concepts in the diagnosis and management of cytokine release syndrome. *Blood* **124**, 188–195 (2014).

Acknowledgments: We thank J. Zhao for comments on and editing of this paper. Editorial services were provided by N. R. Gough (BioSerendipity LLC). **Funding:** X.Y. was supported by The National Key Research and Development Program of China (2016YFC1303400), National Natural Science Foundation of China (81971467 and 81671643), and Shanghai Jiao Tong University Scientific and Technological Innovation Funds. J.C. was supported by Jiangsu Province Social Development Key Projects (BE2017639). The research was funded in part by Shanghai Longyao Biotechnology Limited. **Author contributions:** X.Y. and J.C. designed the clinical trial. X.Y., Y.-X.F., H.Z., F.L., and J.C. designed the overall project. H.Z., F.L., J.C., X.W., G.W., H.C., K.Q., K.X., J.Z., and X.Y. performed the experiments. J.C., X.W., H.C., K.Q., K.X., and J.Z. performed the clinical trial. H.Z., F.L., Y.-X.F., and X.Y. analyzed the results and wrote the manuscript. **Competing interests:** X.W. is an employee of Shanghai Longyao Biotechnology Limited. X.Y. is a consultant of Shanghai Longyao Biotechnology Limited. All other authors declare that they have no competing interests. Shanghai Longyao Biotechnology Limited has filed a patent (application no. 201810636409.0) related to this study with X.Y., Y.-X.F., X.W., H.Z., and F.L. listed as inventors. **Data and materials availability:** All data associated with this study are present in the paper or the Supplementary Materials. All the tumor cell lines and plasmids used in this study will be made available for the scientific community through contacting the corresponding author and completion of a material transfer agreement.

Submitted 1 January 2020
Resubmitted 24 August 2020
Accepted 20 November 2020
Published 27 January 2021
10.1126/scitranslmed.aba7308

Citation: H. Zhang, F. Li, J. Cao, X. Wang, H. Cheng, K. Qi, G. Wang, K. Xu, J. Zheng, Y.-X. Fu, X. Yang, A chimeric antigen receptor with antigen-independent OX40 signaling mediates potent antitumor activity. *Sci. Transl. Med.* **13**, eaba7308 (2021).

Science Translational Medicine

A chimeric antigen receptor with antigen-independent OX40 signaling mediates potent antitumor activity

Huihui Zhang, Fanlin Li, Jiang Cao, Xin Wang, Hai Cheng, Kunming Qi, Gang Wang, Kailin Xu, Junnian Zheng, Yang-Xin Fu and Xuanming Yang

Sci Transl Med **13**, eaba7308.
DOI: 10.1126/scitranslmed.aba7308

Optimizing with OX40

Chimeric antigen receptor (CAR)–T cells have transformed treatment of B cell malignancies. However, existing CAR-T cell constructs have not been as successful in treating solid tumors. To improve CAR-T cell function in solid tumors, Zhang *et al.* incorporated a full-length costimulatory signaling molecule, OX40, into CAR-T cells. The combination of CAR signaling and OX40 signaling improved the antitumor cytolytic capacity of CAR-T cells in vitro and in mouse models of B cell lymphoma. Further, in a phase 1 clinical trial, the authors showed that CAR-T cells expressing OX40 persist in patients with metastatic lymphoma, are well tolerated, and reduce tumor burden. These findings suggest that CAR-T cells with independent OX40 signaling may be a useful therapeutic approach to treat solid tumors.